Image Processing

References:

1. Ballard & Brown, Computer Vision
2. Gonzalez & Woods, Digital Image Processing, 2/e
3. Kelly, Robot Vision

Unretouched cable picture of Generals Pershing and Foch, transmitted by tone equipment from London to New York. (From McFarlane [1972].)

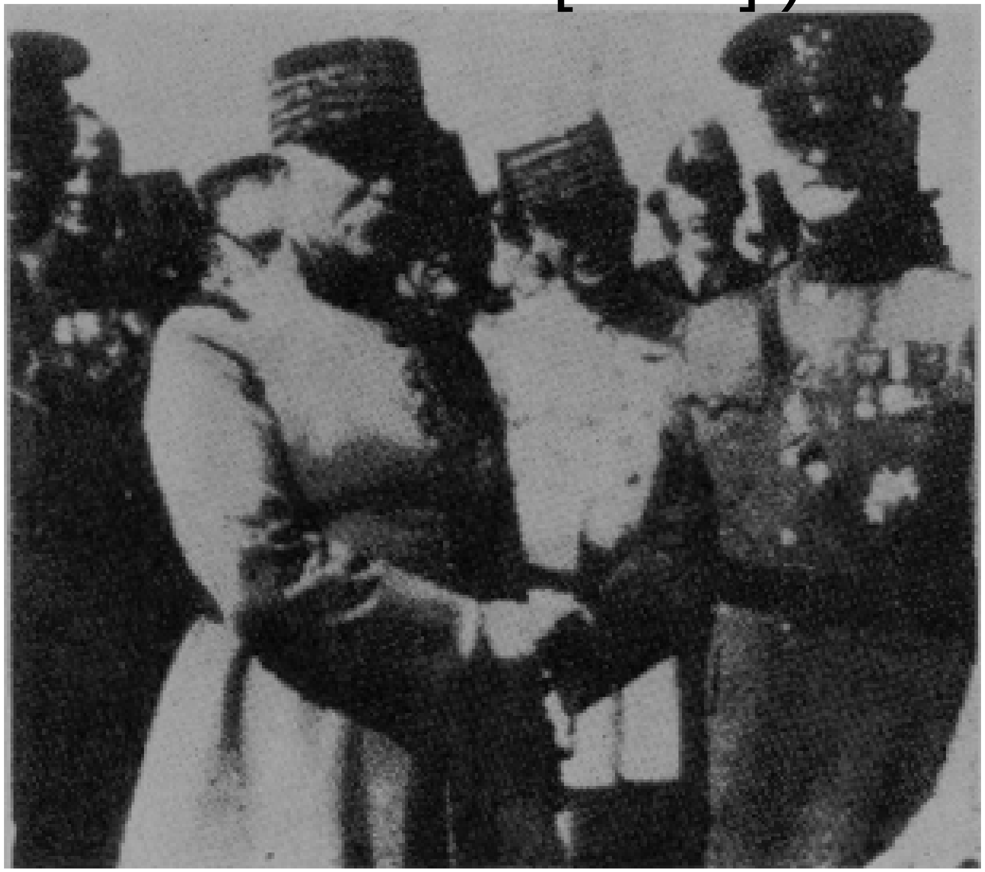

NASA Image of Jupiter

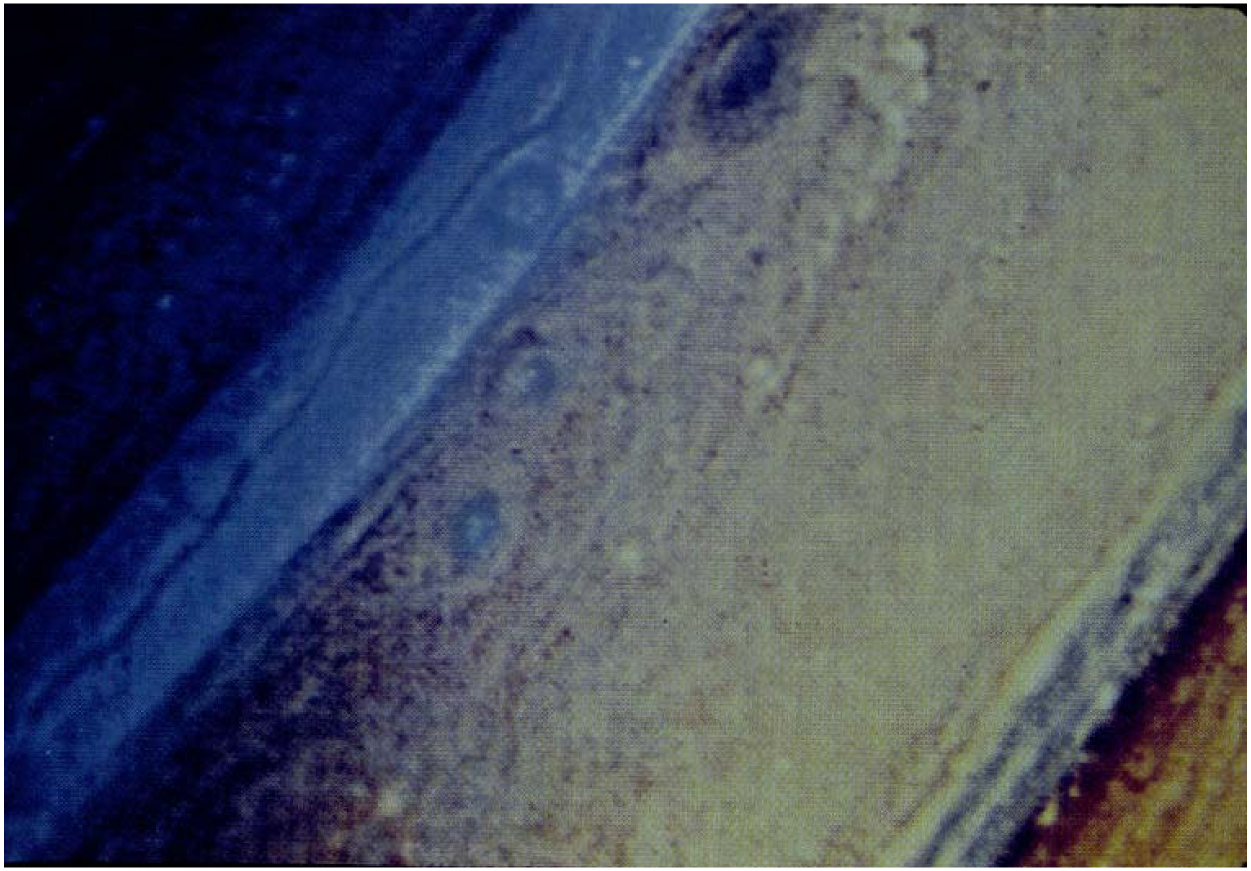

- Pseudocolors differentiate between vegetation, pavement and buildings, and graphic plane overlays plot property lines.

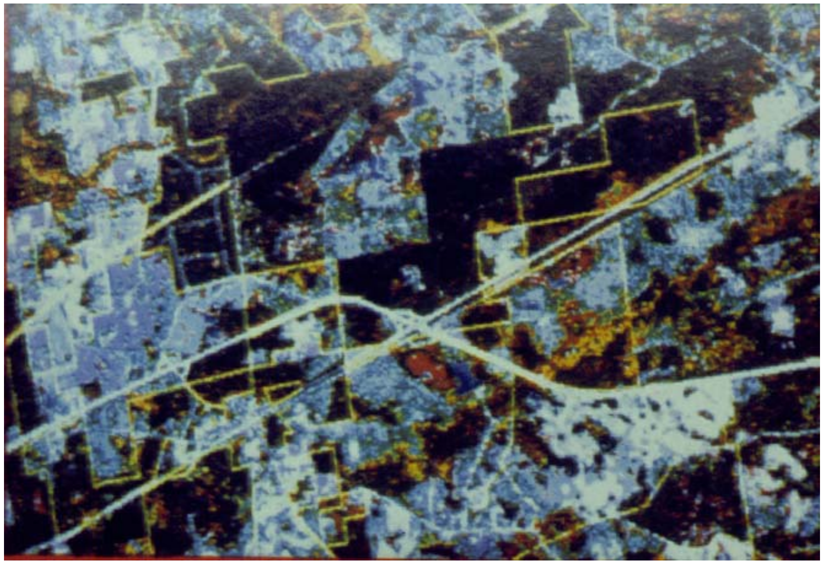

Detail not evident in the original, left, is brought out by high pass laplacian filtering, right.

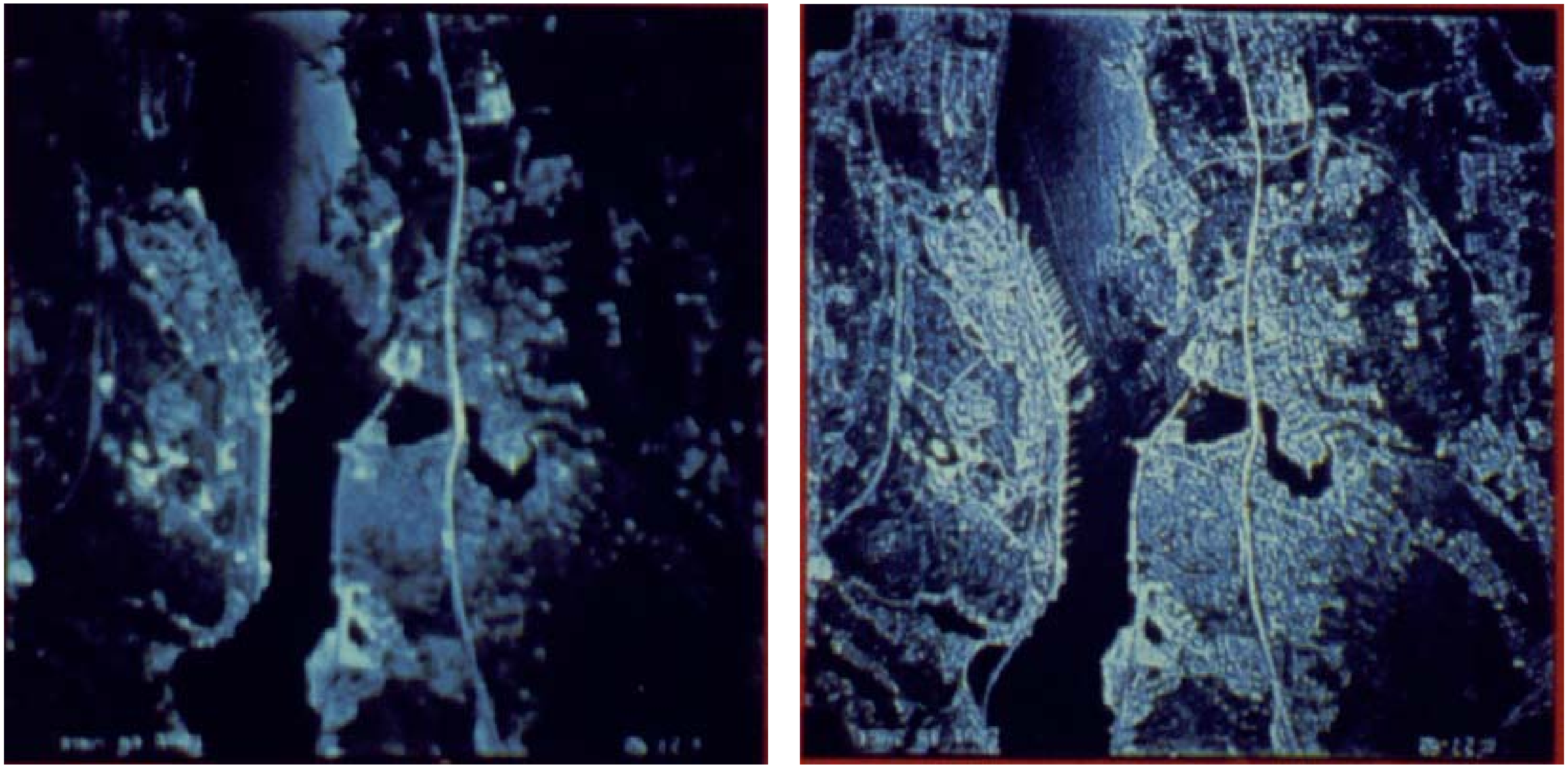

2X zoom provides detail, left, while filtering reveals tire tracks, right.

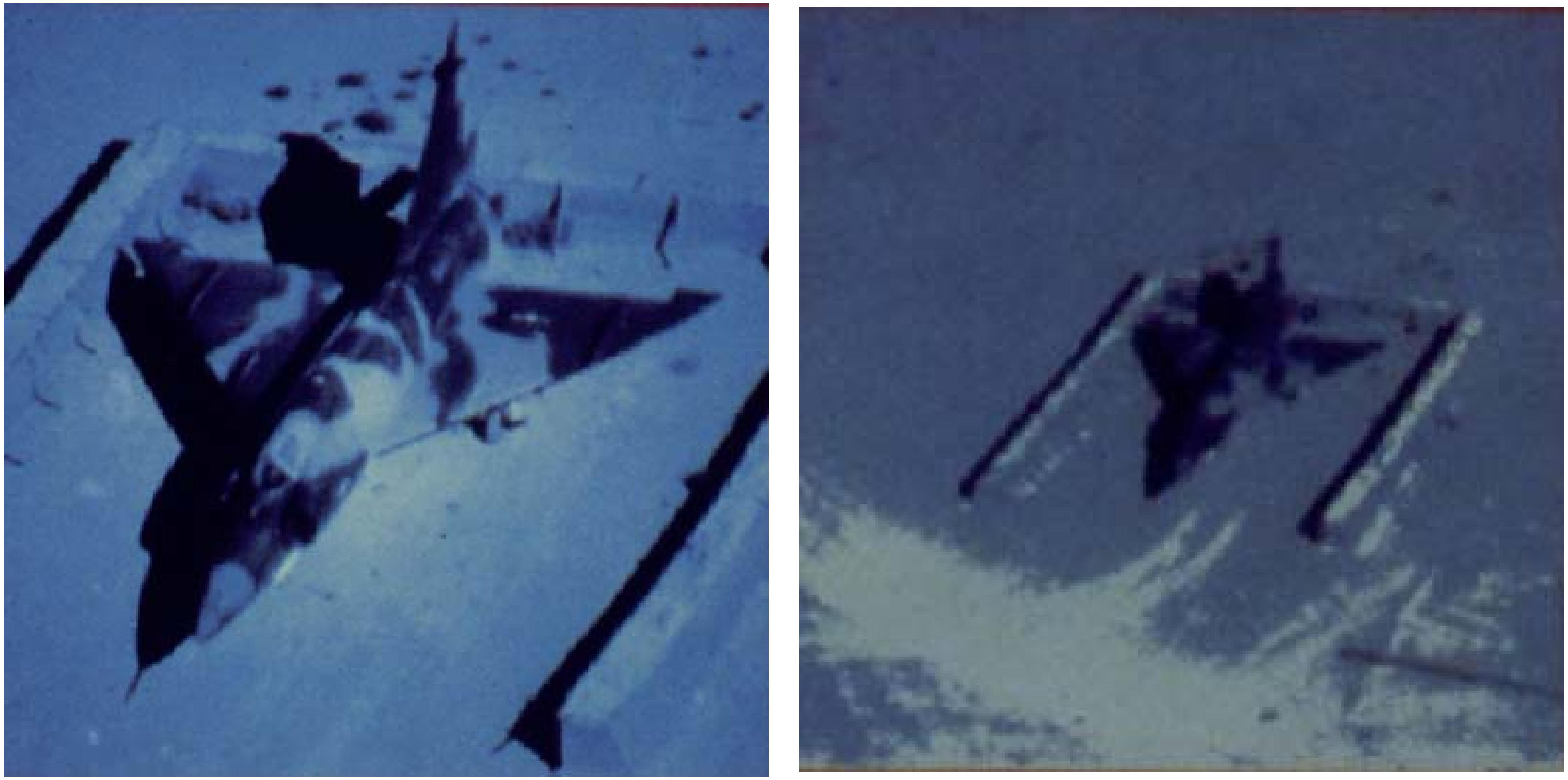

Three-dimensional machine vision system performs 100-percent inspection of mass-produced stamped metals parts without human assistance. In the system, developed by Perceptron, Inc. of Farmington Hills, Mich., a sensor, camera, and light source are mounted at a fixed angular relationship and distance. Introduction of a part into the field of view shifts the position of the reflected light beam on the imaging cells of the camera. Using high-speed triangulation, the system's microcomputer determines the parts contour to within 0.0001 inch.

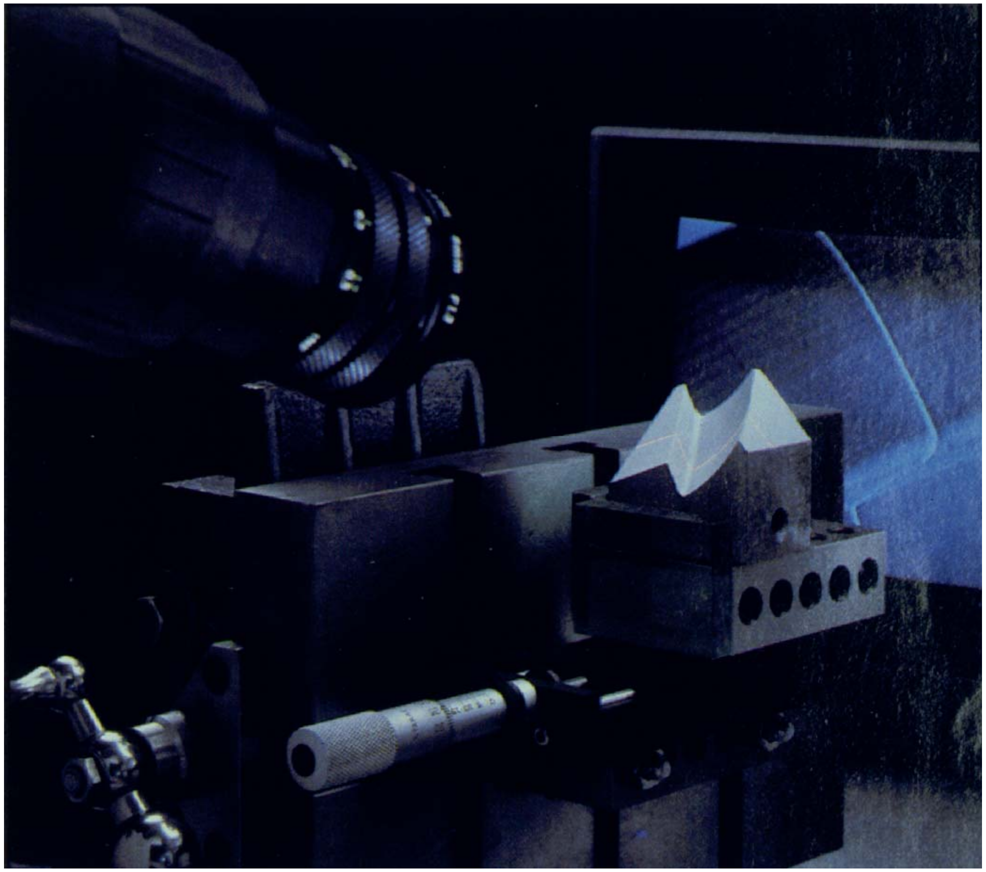

[1] An automatic milling machine with a loading-unloading robot relies on diverse sensors, actuators, and displays. On the machine tool, dc motors (1) provide movement on the x, y, and z axes; tachometers (2) sense the speeds of the axis motors; resolvers (3) sense axis-motor shaft position; an ac motor (4) drives the tool spindle; and limit switches (5) sense when the milling table is approaching its maximum allowable bounds and thus prevent overtravel. A stepping motor (6) positions the tool changer so that the spindle can accept a new tool at the appropriate moment, and a tactile probe (7) measures the dimensions of the workpiece at each machining step. In the machine-control unit, servo amplifiers (8) regulate the machine drives, a computer (9) exercises overall control, and a display (10) keeps a human supervisor informed of the machine status. On the robot, hydraulic servo valves (11) actuate the arm, optical encoders (12) sense the position of the arm, a pneumatic control valve (13) actuates the robot's gripper, and a tactile sensor (14) measures the gripper force. The robot control contains servo amplifiers (15), a computer (16), and a display (17). Overhead, a TV camera (18) identifies parts and guides the robot.

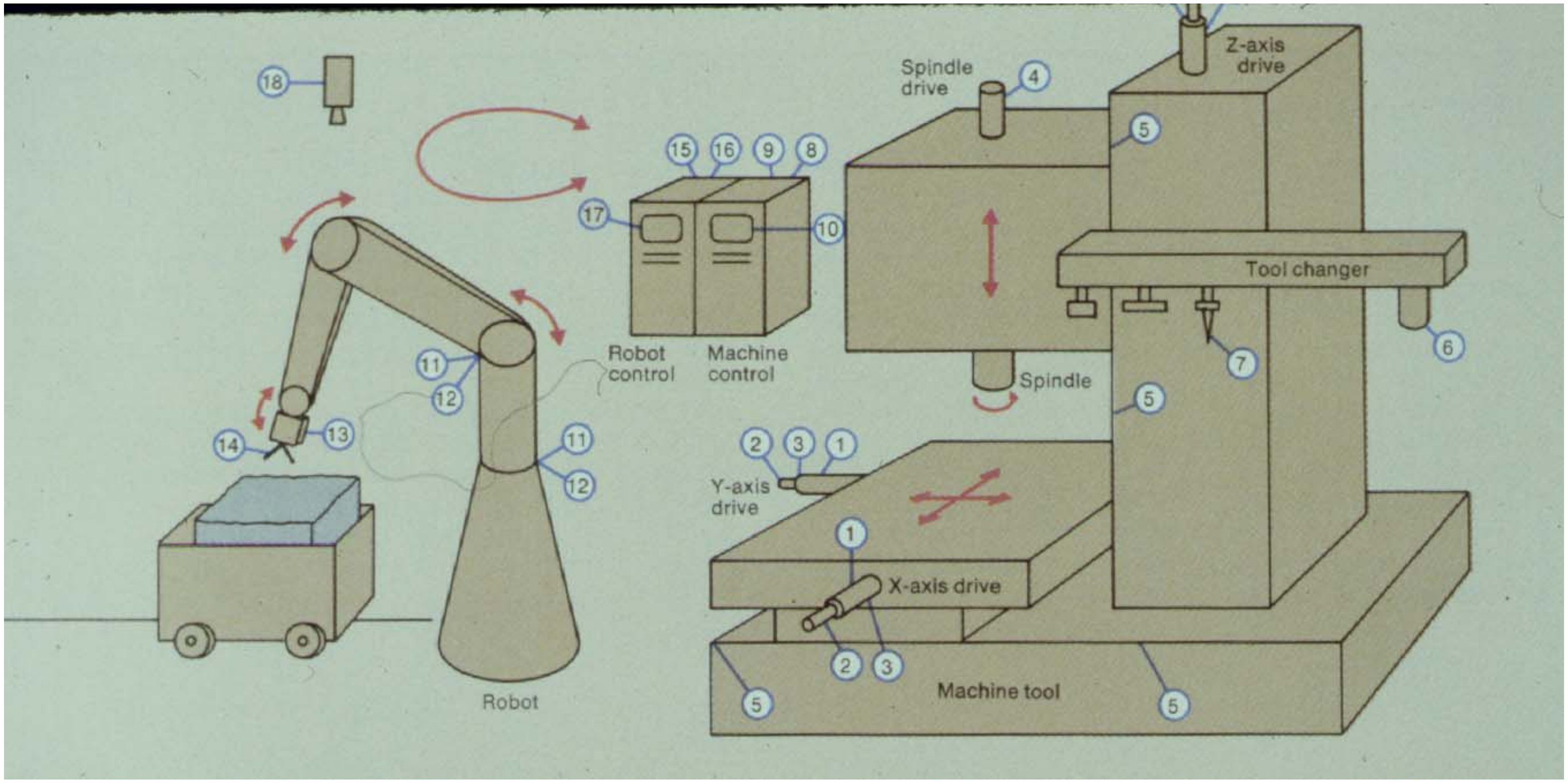

Vision guided robot used for nuclear reactor repairs.

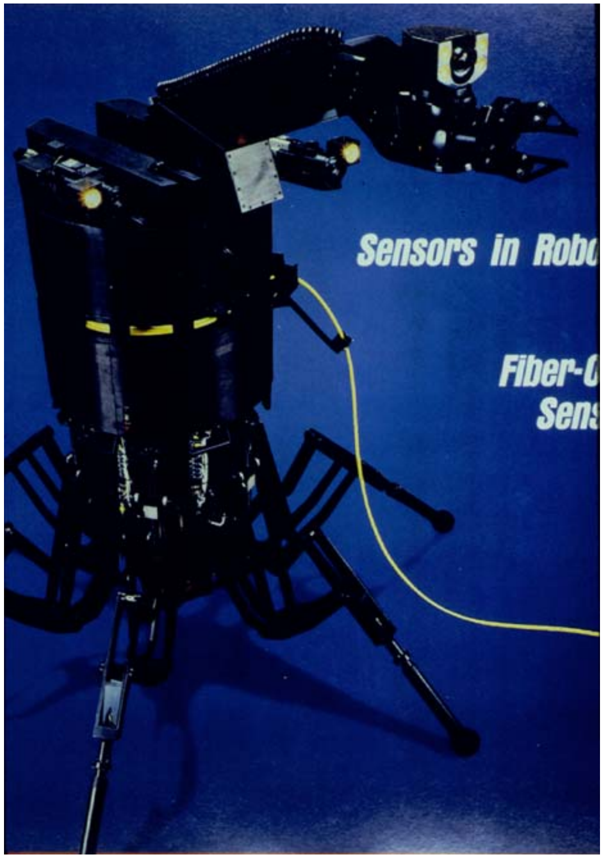

Robotic vehicles

ENSCO Vision guided robotic vehicle for DARPA Grand Challenge

A computed tomography scan reconstructed image. High-resolution computed tomography shown here is being used to diagnose the causes of lower back pain. (Used with permission from Technicare Corp., 1982).

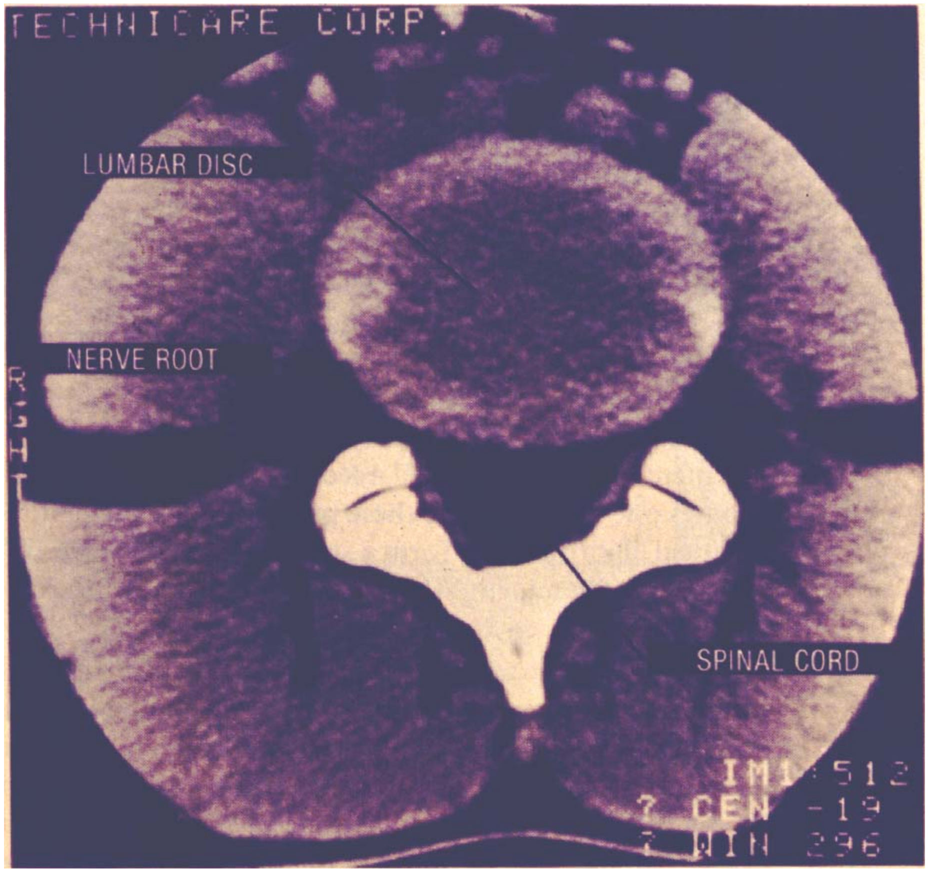

Colorization

Computer enhanced images

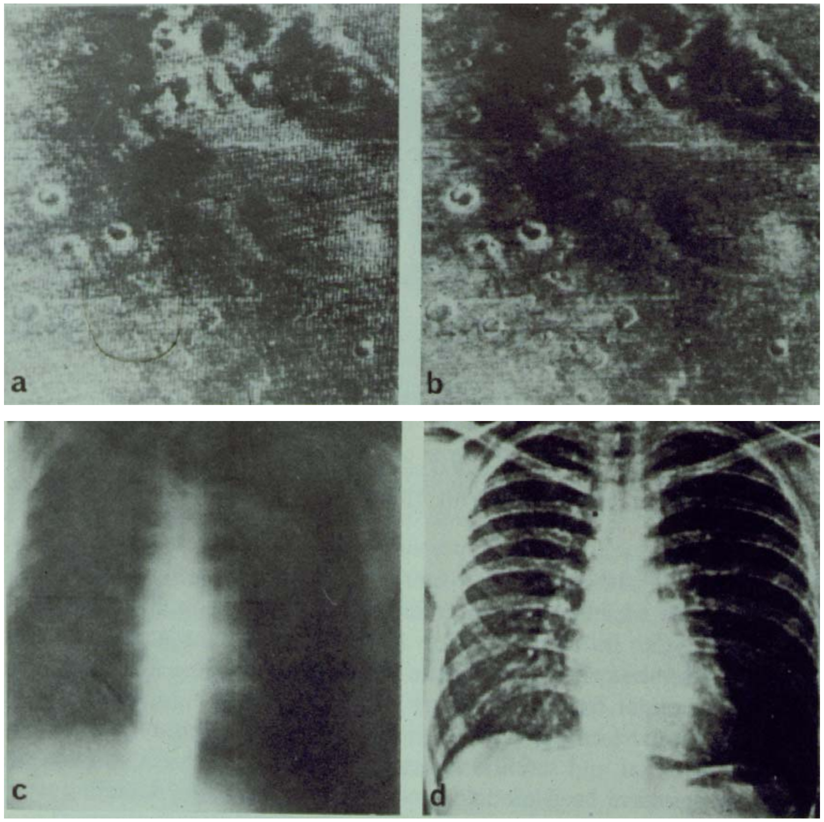

(a) and (b) represent a sharpened image;

(c) and (d) show the result of histogram equalization;

(e) and (f) show the result of motion compensation.

? images

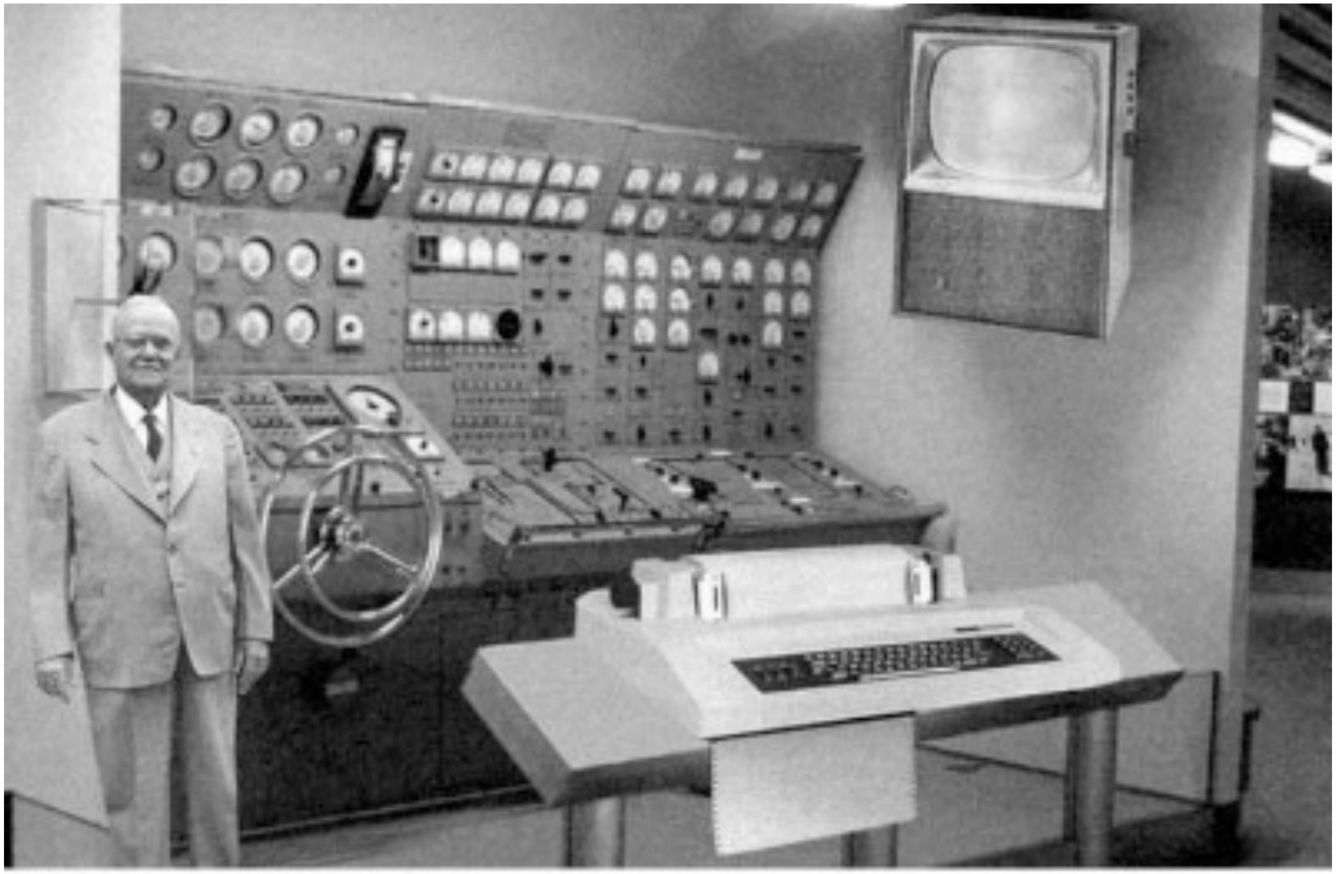

Scientists from the RAND Corporation have created this model to illustrate how a "home computer" could look like in the year 2004. However the needed technology will not be economically feasible for the average home. Also the scientists readily admit that the computer will require not yet invented technology to actually work, but 50 years from now scientific progress is expected to solve these problems. With teletype interface and the Fortran language, the computer will be easy to use.

Elements of a digital image processing system.

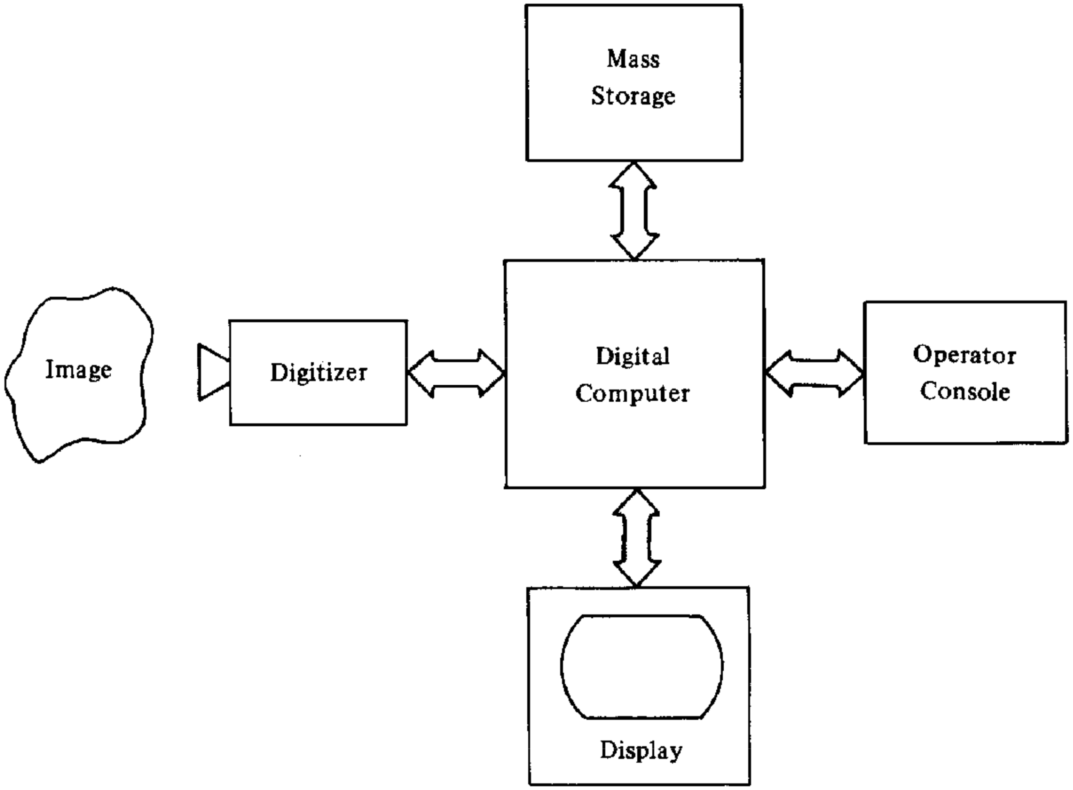

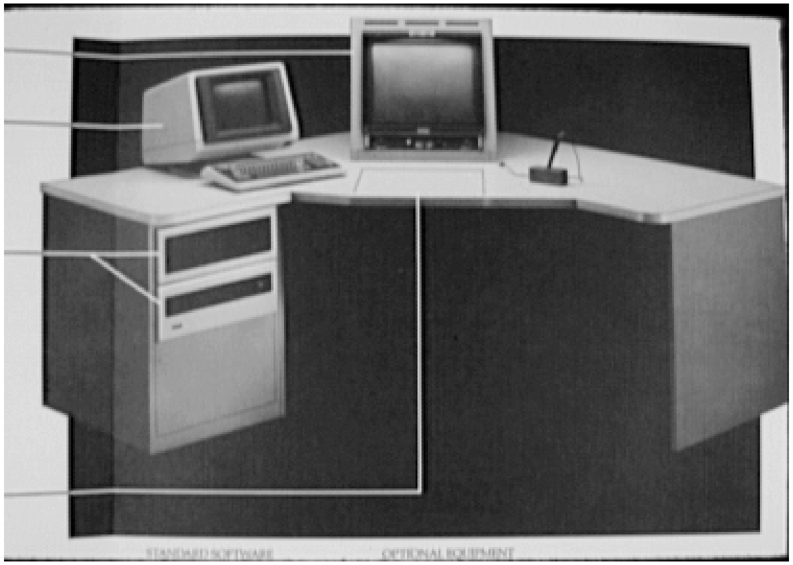

STANDARD SOFTWARE

OPTIONAL EQUIPMENT

IP often uses specialized hardware

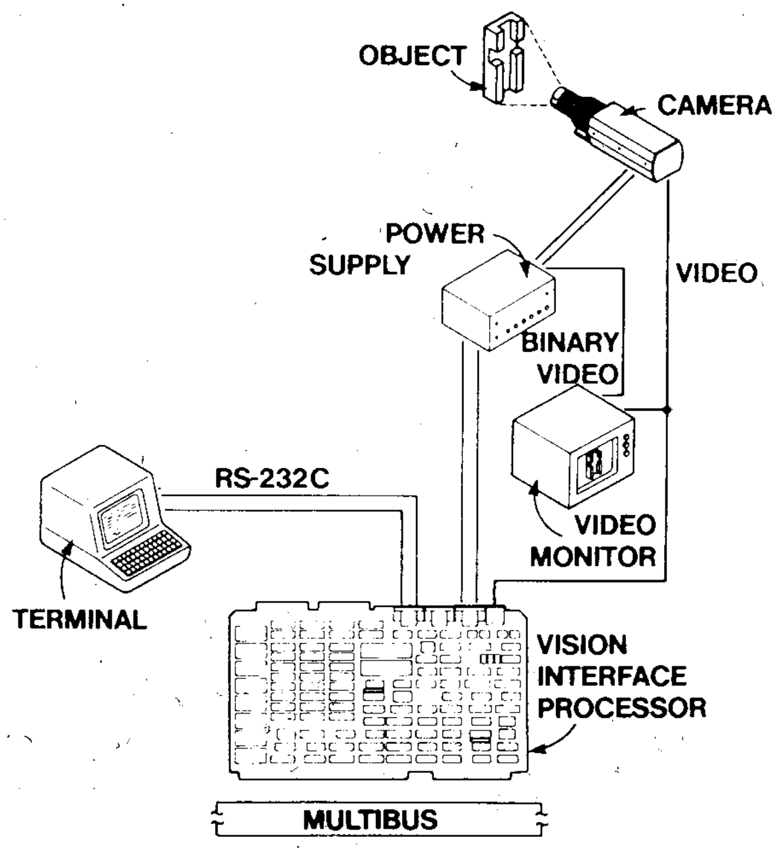

Physiological basis of vision/image processing

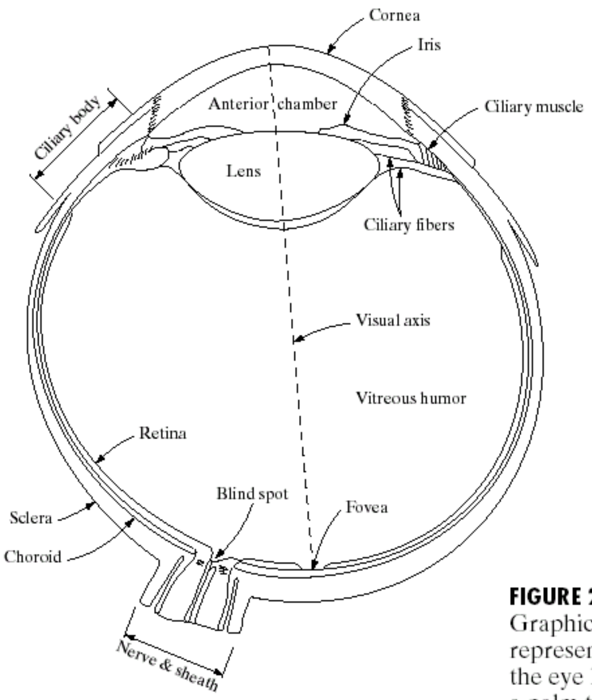

FIGURE 2.1 Simplified diagram of a cross section of the human eye.

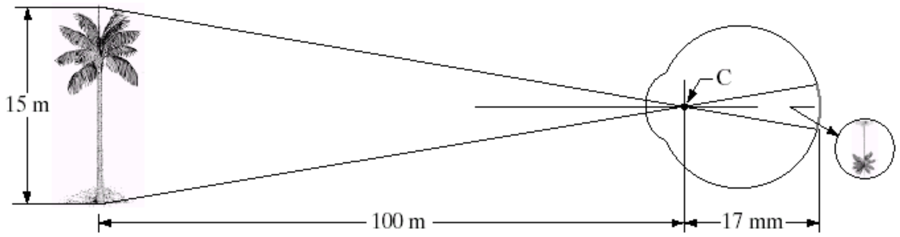

FIGURE 2.3 Graphical representation of the eye looking at a palm tree. Point *C* is the optical center of the lens.

Typical Model for Image Acquisition

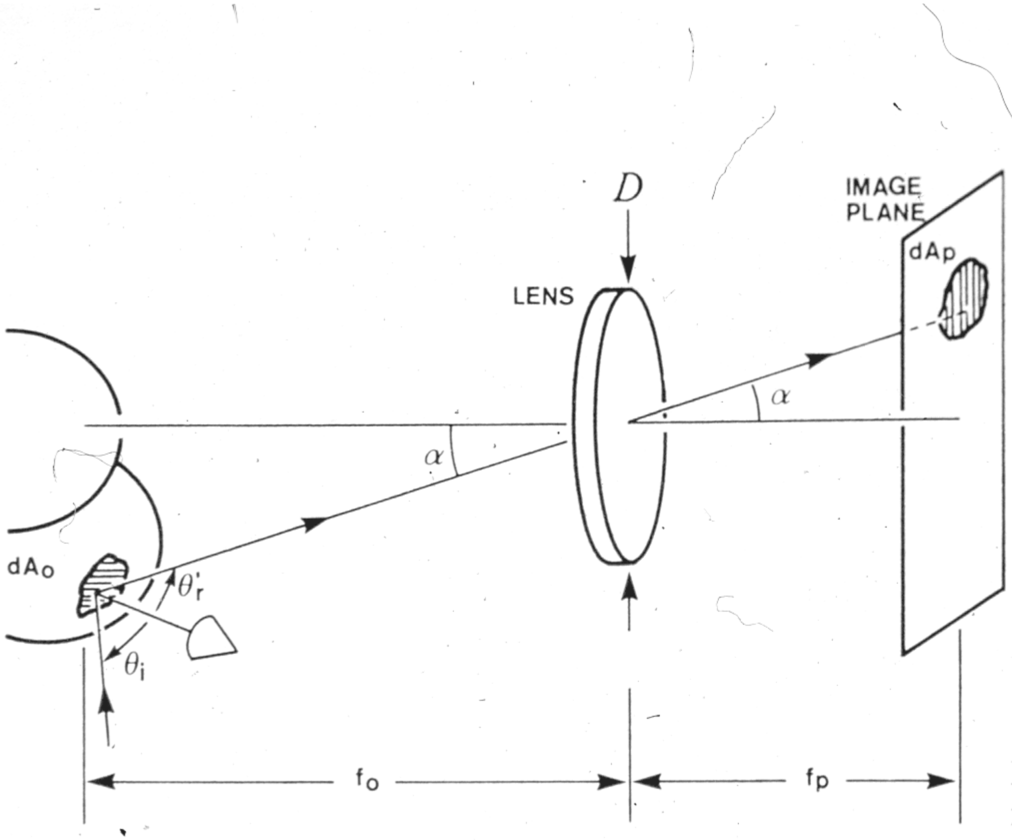

Fig. 2.4 Geometry of an image forming system.

Geometric Camera Models

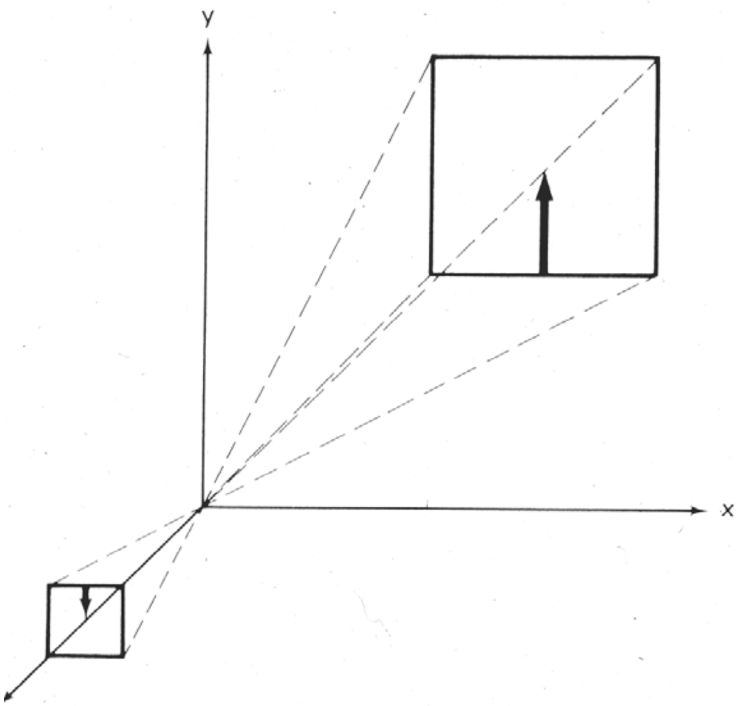

Fig. 2.1 A geometric camera model.

Homogeneous Coordinate Transformation

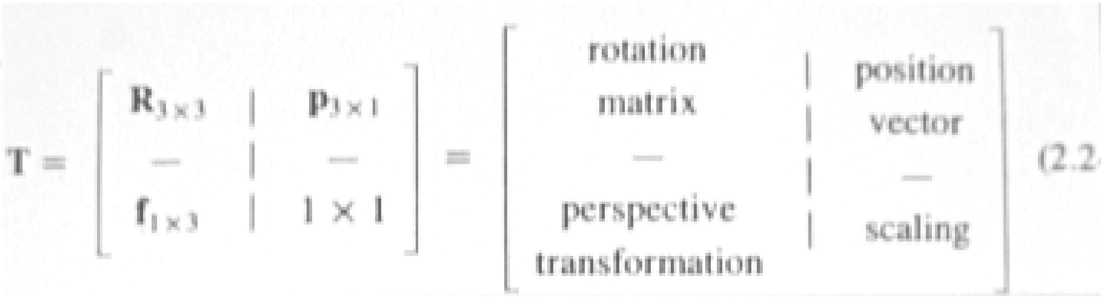

$$\mathbf{T} = \left[\begin{array}{c|c} \mathbf{R}_{3\times 3} & \mathbf{p}_{3\times 1} \\ - & - \\ \mathbf{f}_{1\times 3} & 1\times 1 \end{array}\right] = \left[\begin{array}{c|c} \text{rotation} & \text{position} \\ \text{matrix} & \text{vector} \\ - & - \\ \text{perspective} & \text{scaling} \\ \text{transformation} & \end{array}\right] \quad (2.2$$

Computer Image Representation

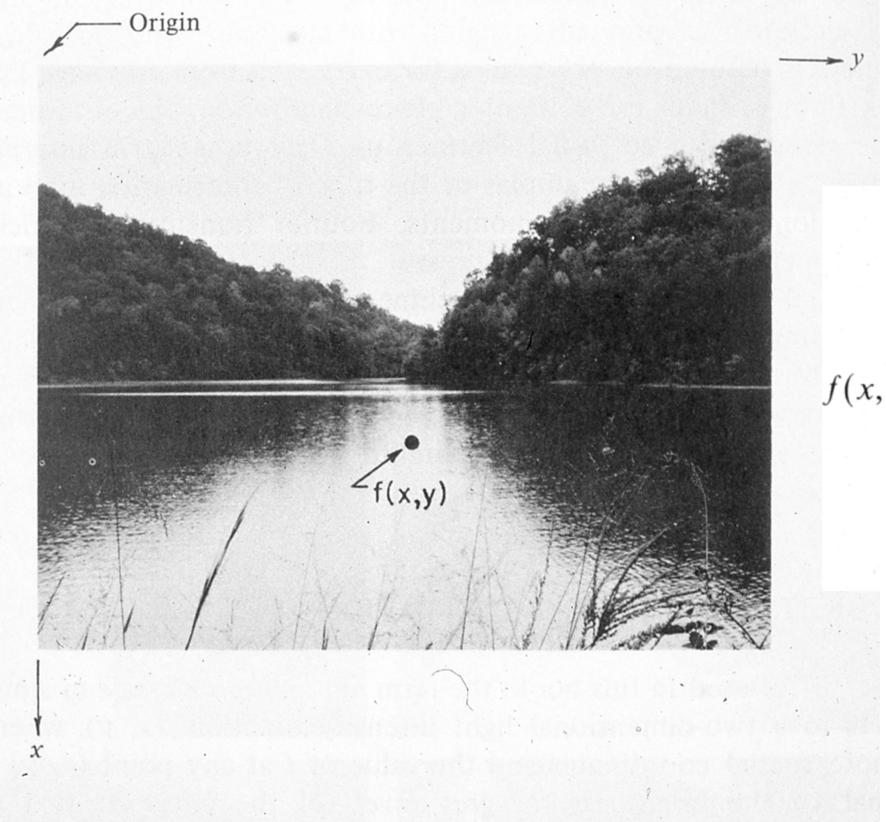

Figure 1.5. Axis convention used for digital image representation.

$$f(x,y) \approx \begin{bmatrix} f(0,0) & f(0,1) & \cdots & f(0,N-1) \\ f(1,0) & f(1,1) & \cdots & f(1,N-1) \\ \vdots & & & \\ f(N-1,0) & f(N-1,1) & \cdots & f(N-1,N-1) \end{bmatrix}$$

Image Representation

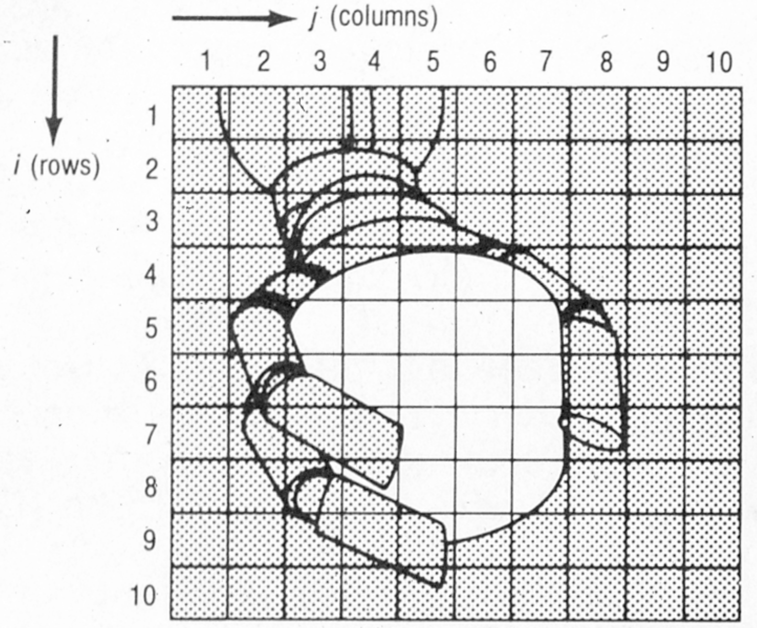

i (rows) ↓ · j (columns) →

	1	2	3	4	5	6	7	8	9	10
1	45	78	35	34	41	40	74	121	126	128
2	42	67	12	27	31	44	66	115	129	124
3	40	63	28	25	20	27	59	109	117	126
4	62	74	49	110	136	145	138	102	112	115
5	124	103	77	226	238	243	240	104	109	191
6	127	117	69	109	221	230	225	109	101	107
7	130	127	66	78	118	210	205	93	85	103
8	134	134	85	73	129	175	190	125	99	100
9	138	135	133	199	80	94	98	104	105	108
10	139	136	133	129	126	122	112	119	139	171

Figure 9.1 Digitized picture with 10 x 10 pixels and the digitized results (from Eskenazi [12]).

0=black; 255=white

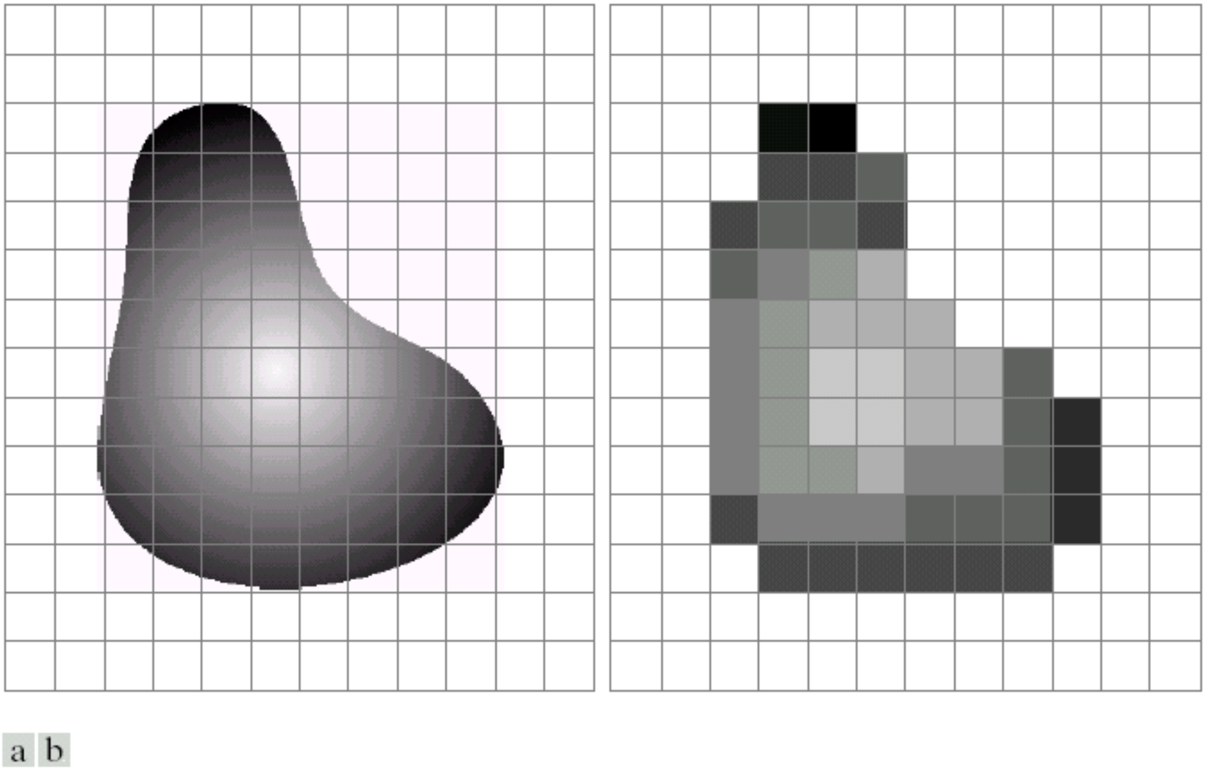

FIGURE 2.17 (a) Continuos image projected onto a sensor array. (b) Result of image sampling and quantization.

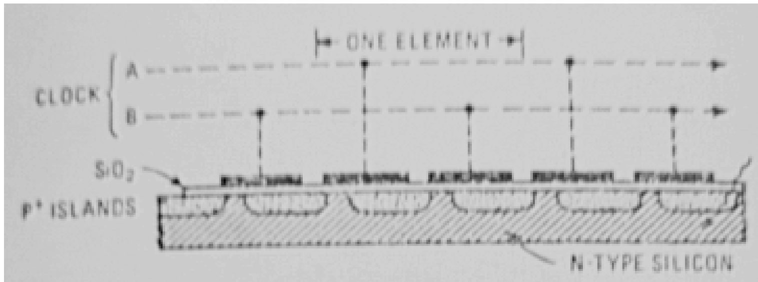

Fig. 2.2

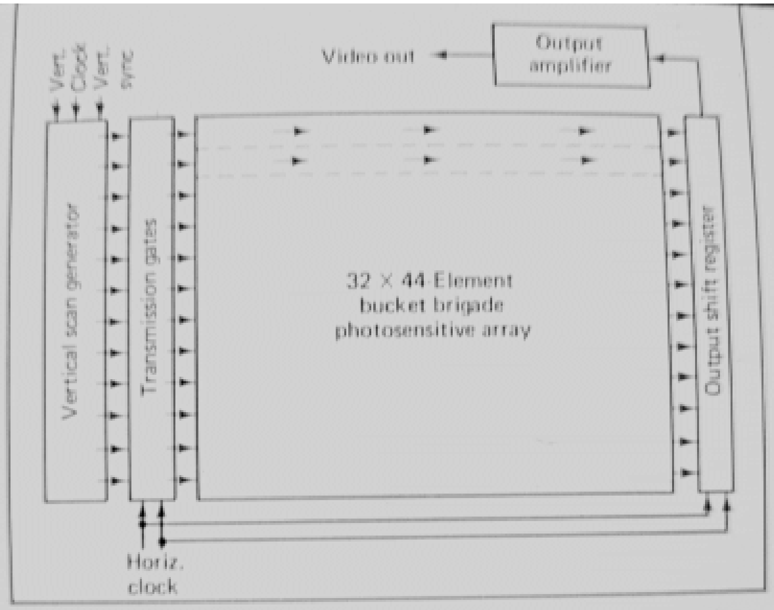

Fig. 2.23 A CCD array (line transfer).

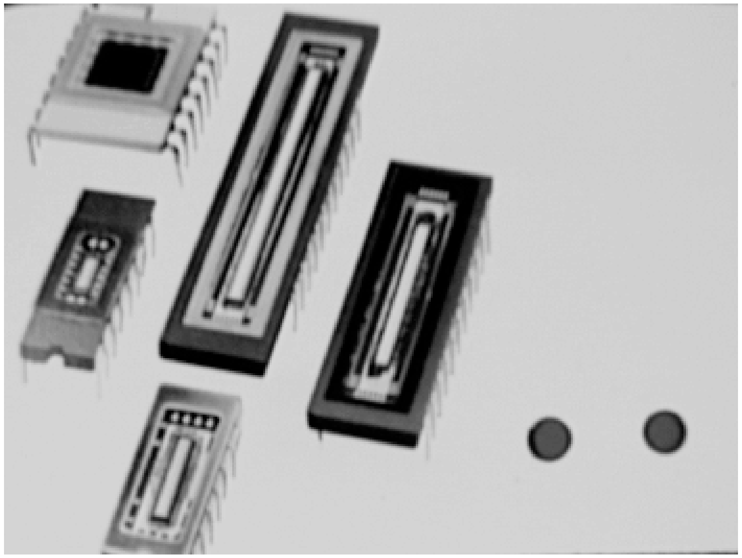

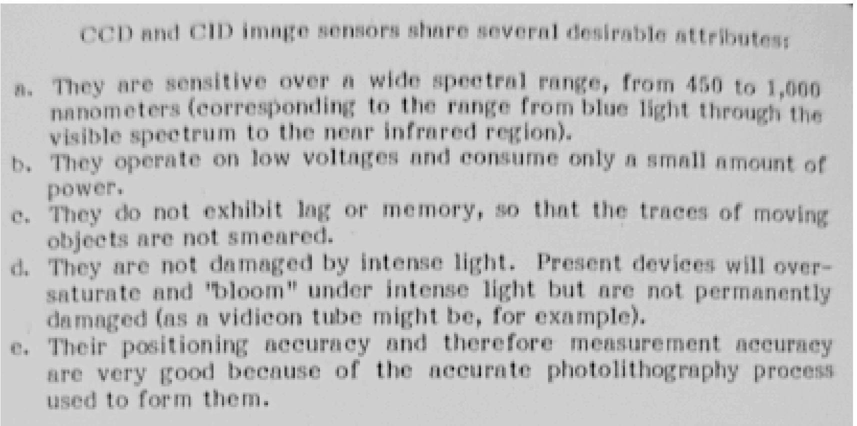

CCD and CID image sensors share several desirable attributes:

a. They are sensitive over a wide spectral range, from 450 to 1,000 nanometers (corresponding to the range from blue light through the visible spectrum to the near infrared region).
b. They operate on low voltages and consume only a small amount of power.
c. They do not exhibit lag or memory, so that the traces of moving objects are not smeared.
d. They are not damaged by intense light. Present devices will oversaturate and "bloom" under intense light but are not permanently damaged (as a vidicon tube might be, for example).
e. Their positioning accuracy and therefore measurement accuracy are very good because of the accurate photolithography process used to form them.

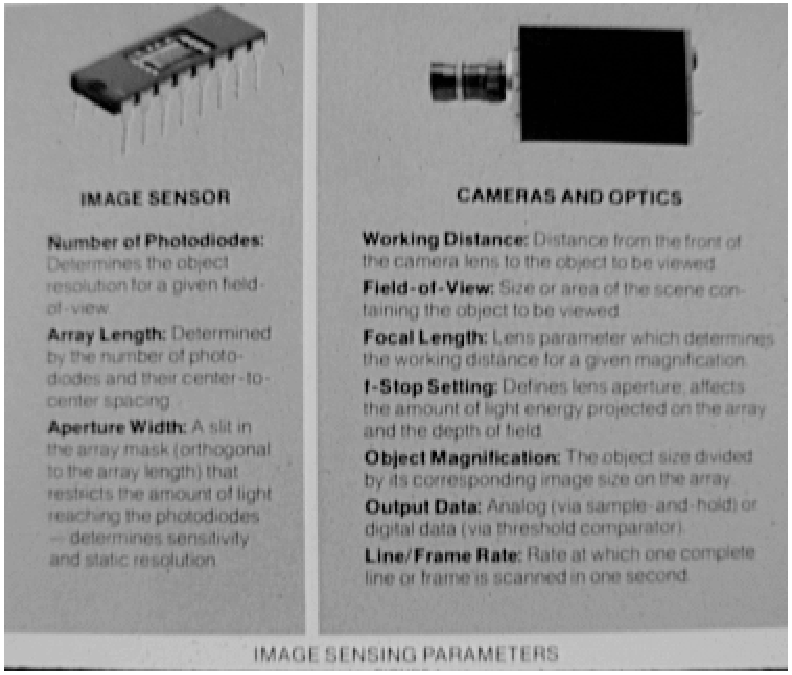

IMAGE SENSOR

Number of Photodiodes: Determines the object resolution for a given field-of-view.

Array Length: Determined by the number of photodiodes and their center-to-center spacing.

Aperture Width: A slit in the array mask (orthogonal to the array length) that restricts the amount of light reaching the photodiodes — determines sensitivity and static resolution.

CAMERAS AND OPTICS

Working Distance: Distance from the front of the camera lens to the object to be viewed.

Field-of-View: Size or area of the scene containing the object to be viewed.

Focal Length: Lens parameter which determines the working distance for a given magnification.

f-Stop Setting: Defines lens aperture; affects the amount of light energy projected on the array and the depth of field.

Object Magnification: The object size divided by its corresponding image size on the array.

Output Data: Analog (via sample-and-hold) or digital data (via threshold comparator).

Line/Frame Rate: Rate at which one complete line or frame is scanned in one second.

IMAGE SENSING PARAMETERS

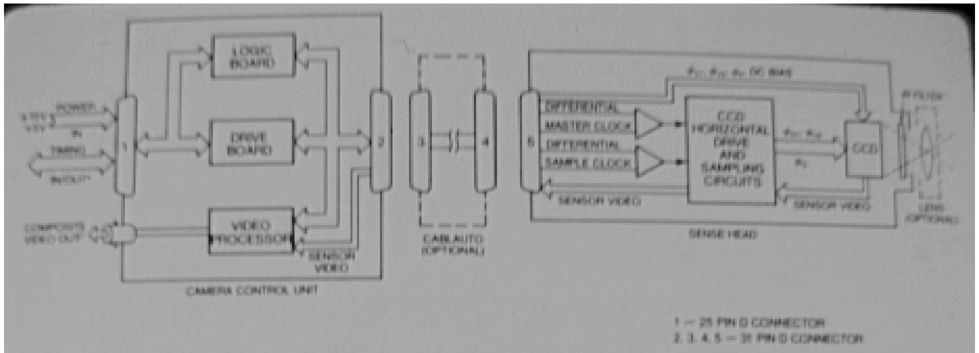

Figure 9.3 Block diagram of a video camera using a CCD area array.

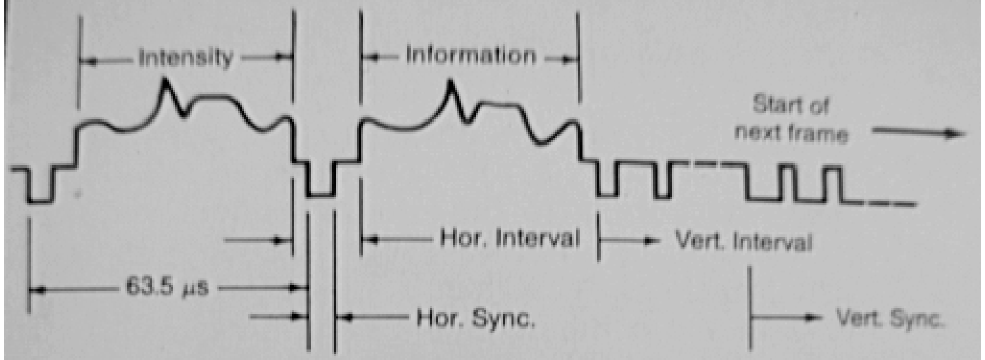

Figure 9.2 Composite video signal to the EIA RS-170 standard.

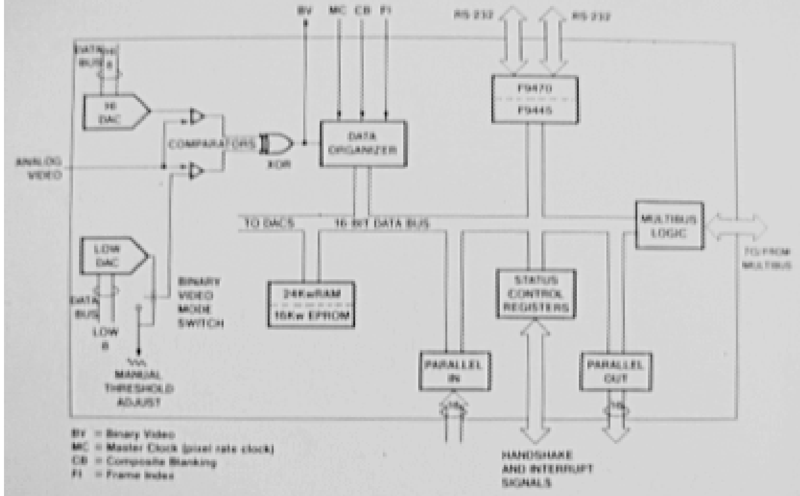

BV = Binary Video
MC = Master Clock (pixel rate clock)
CB = Composite Blanking
FI = Frame Index

Figure 9.5 Block diagram of the vision interface processor (VIP100), Fairchild Corporation.

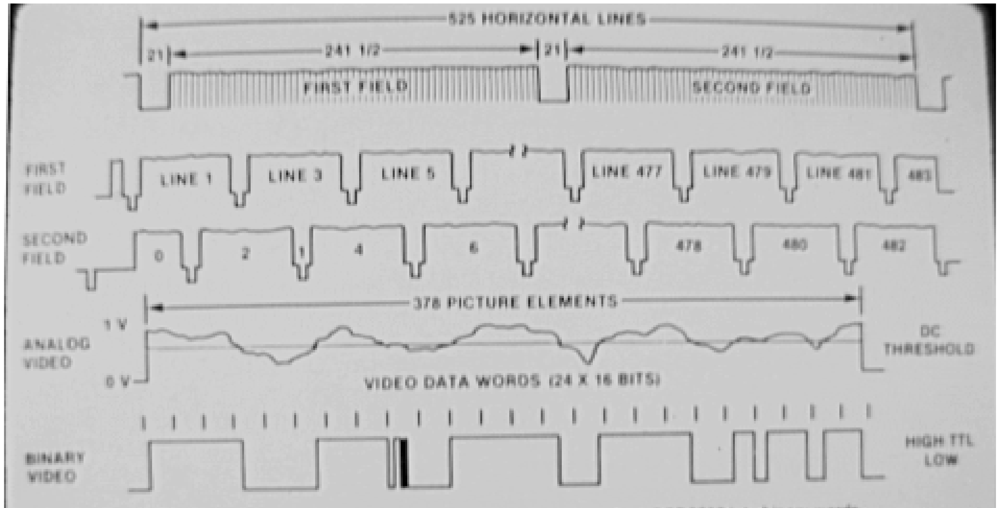

Figure 9.6 Video conversion of image data from CCD3000 into binary words.

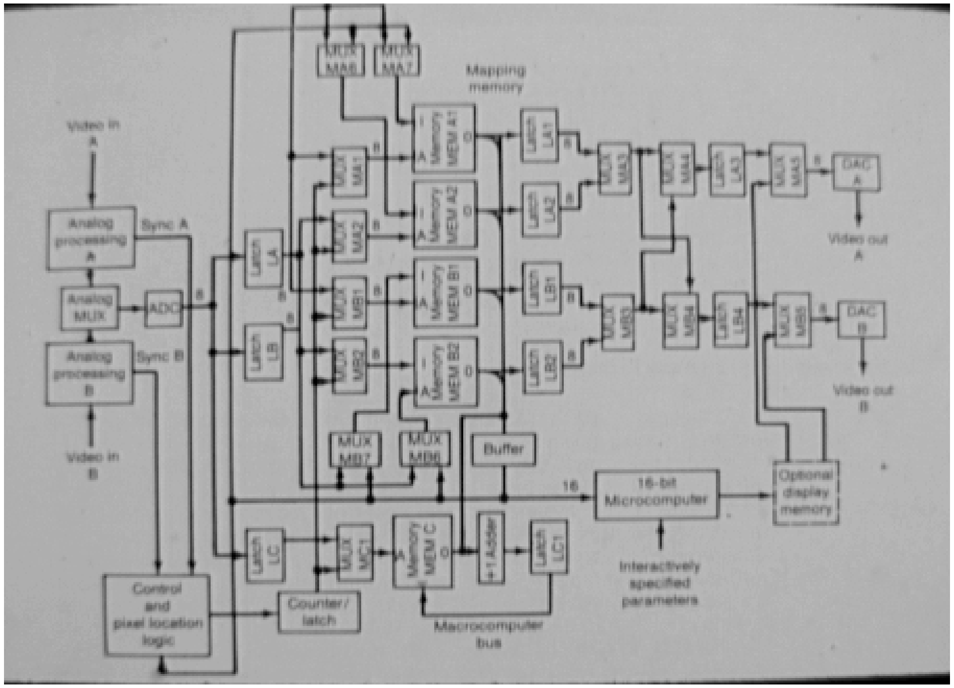
Video in A
Analog processing A
Sync A
Analog MUX
ADC
8
Analog processing B
Sync B
Video in B
Control and pixel location logic
Counter/ latch
Latch LA
Latch LB
Latch LC
MUX MA6
MUX MA7
MUX MA1
MUX MA2
MUX MB1
MUX MB2
MUX MB7
MUX MB6
MUX MC1
Mapping memory
I A Memory MEM A1 O
I A Memory MEM A2 O
I A Memory MEM B1 O
I A Memory MEM B2 O
A Memory MEM C O
Buffer
+1 Adder
Latch LC1
Macrocomputer bus
16
16-bit Microcomputer
Interactively specified parameters
Latch LA1
Latch LA2
Latch LB1
Latch LB2
MUX MA3
MUX MA4
Latch LA3
MUX MA5
MUX MB3
MUX MB4
Latch LB4
MUX MB5
DAC A
DAC B
Video out A
Video out B
Optional display memory

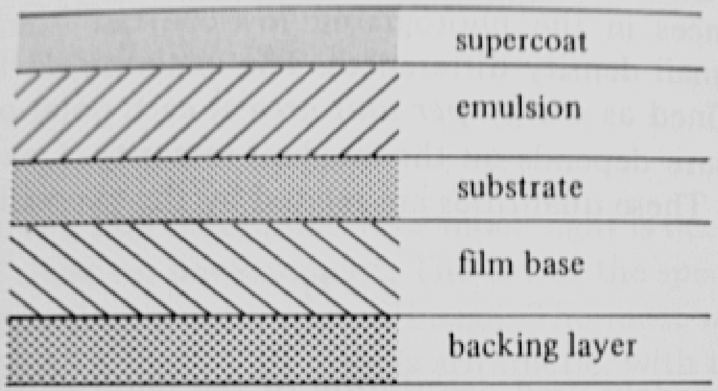

Figure 2.11. Structure of a modern black-and-white film.

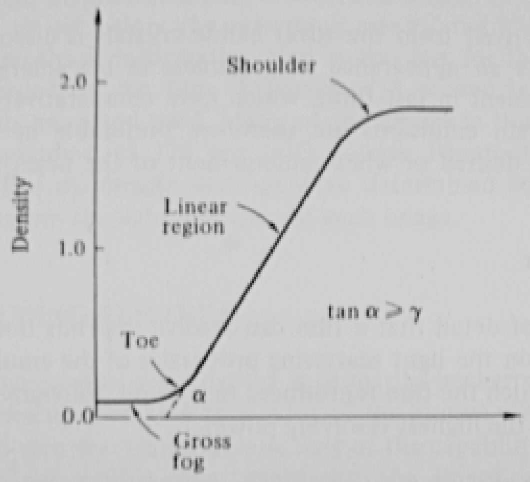

Figure 2.12. A typical *H* & *D* curve.

Spatial Resolution

N=1024

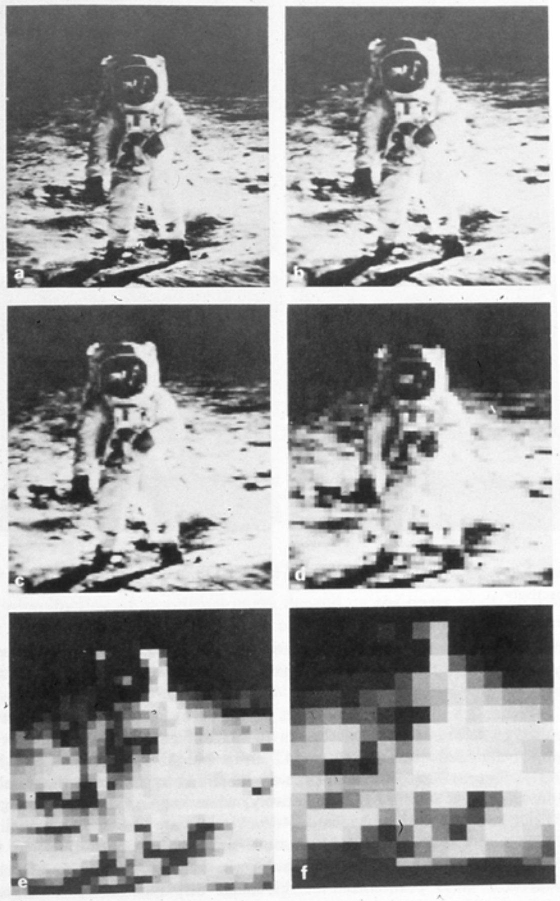

Figure 2.7. Effects of reducing sampling-grid size.

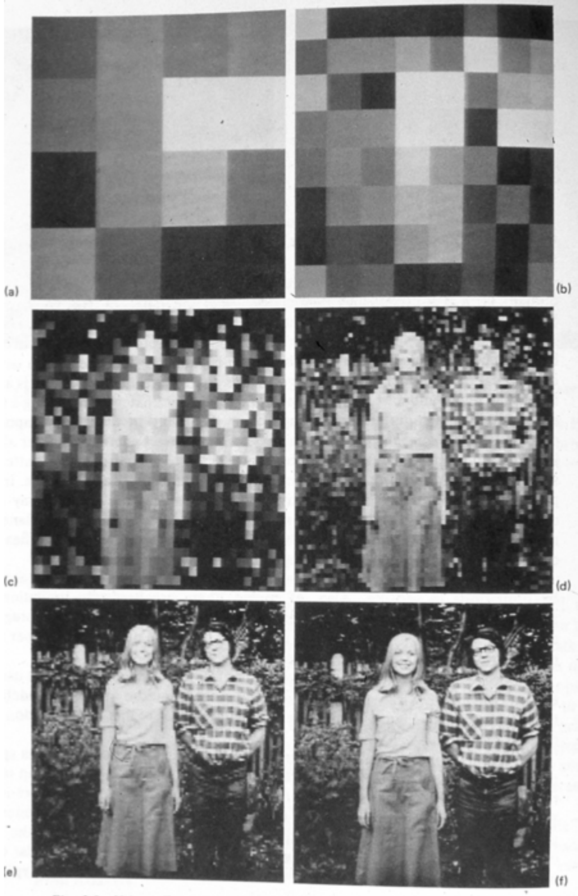

Fig. 2.9 Using different numbers of samples. (a) $N = 16$; (b) $N = 32$; (c) $N = 64$; (d) $N = 128$; (e) $N = 256$; (f) $N = 512$.

N=512

Gray Scale Resolution

N=256

Figure 2.8. A 512 × 512 image displayed in 256, 128, 64, 32, 16, 8, 4, and 2 levels, respectively.

N=2

Gray Scale Resolution

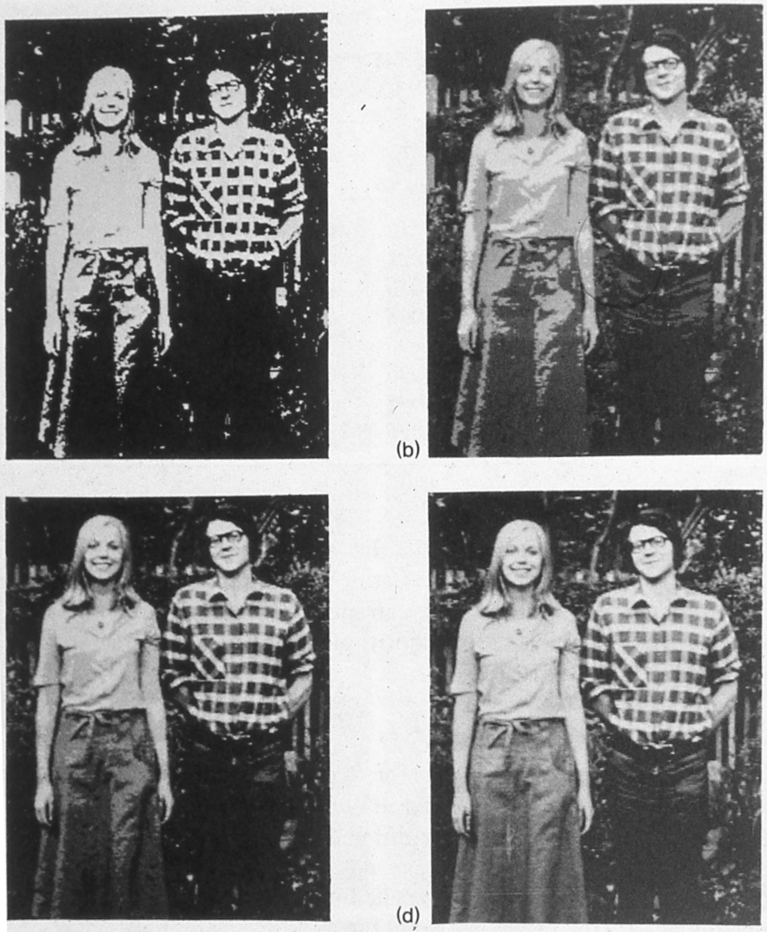

Fig. 2.10 Using different numbers of bits per sample. (a) $m = 1$; (b) $m = 2$; (c) $m = 4$; (d) $m = 8$.

Test Images

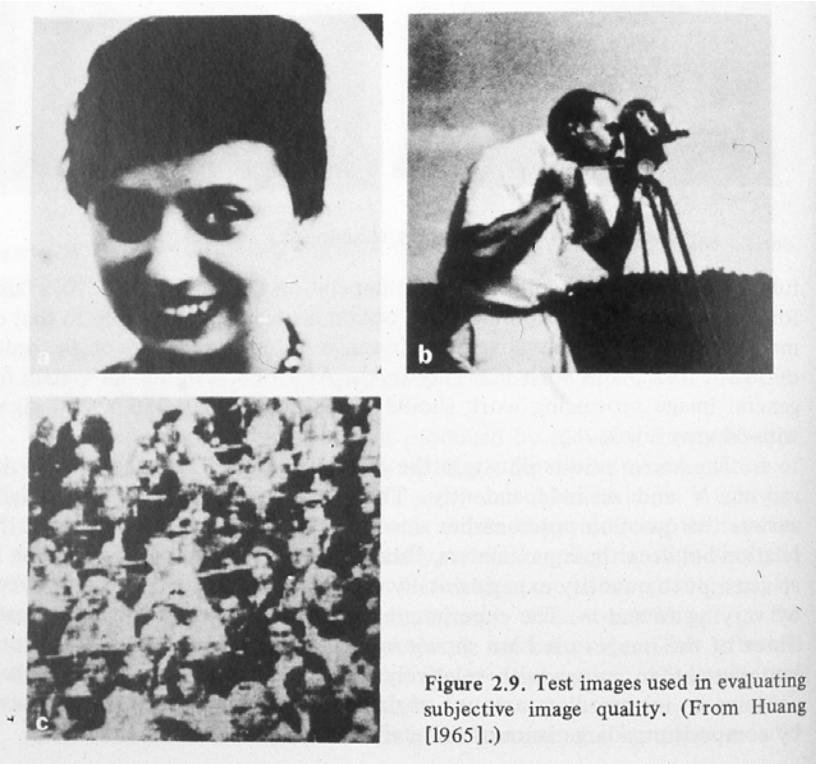

Figure 2.9. Test images used in evaluating subjective image quality. (From Huang [1965].)

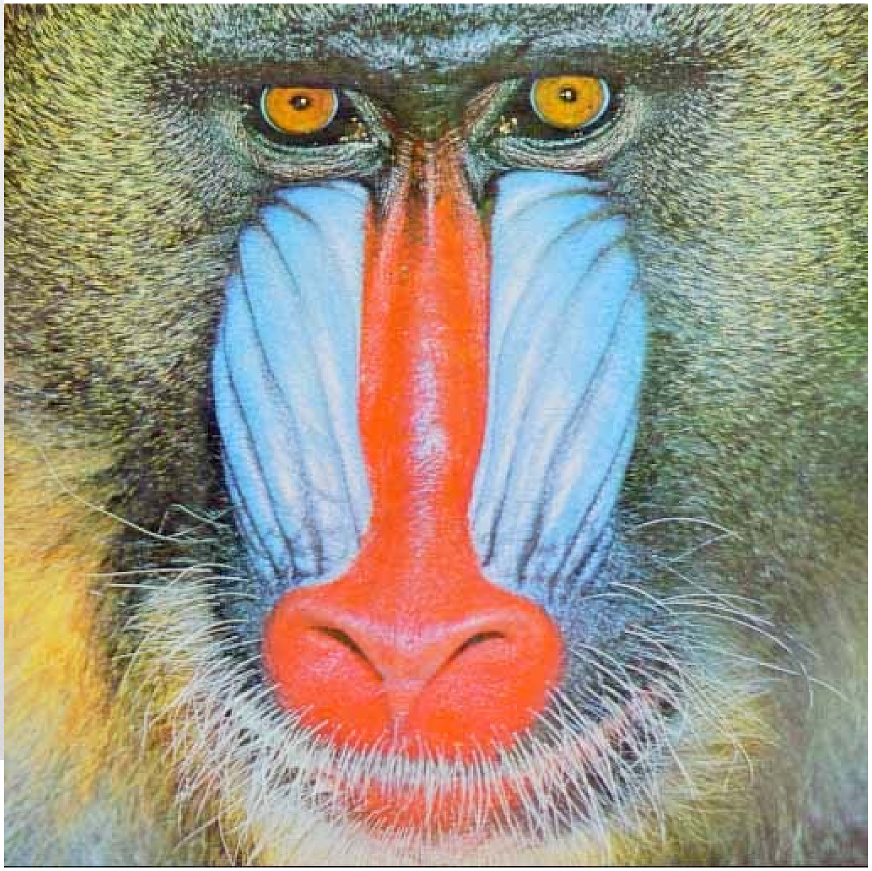

The “Lena” Image

comp.compression FAQ:

For the curious: 'lena' or 'lenna' is a digitized Playboy centerfold, from November 1972. (Lenna is the spelling in Playboy, Lena is the Swedish spelling of the name.) Lena Soderberg (ne Sjooblom) was last reported living in her native Sweden, happily married with three kids and a job with the state liquor monopoly. In 1988, she was interviewed by some Swedish computer related publication, and she was pleasantly amused by what had happened to her picture. That was the first she knew of the use of that picture in the computer business.

A scan of the original Lenna from Playboy is available from http://www.lenna.org

The editorial in the January 1992 issue of Optical Engineering (v. 31 no. 1) details how Playboy has finally caught on to the fact that their copyright on Lena Sjooblom's photo is being widely infringed. However Wired mentioned that: "Although Playboy is notorious for cracking down on illegal uses of its images, it has decided to overlook the widespread distribution of this particular centerfold".

Geometric Transformations

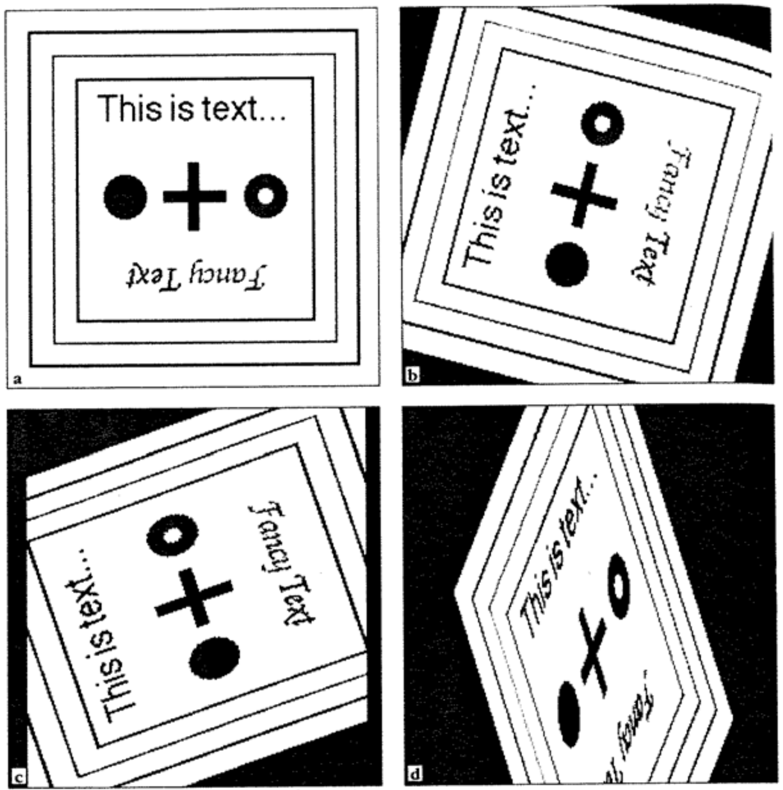

Figure 46. Rotation and stretching of a test image:
a) *original;*
b) *rotation only, no change in scale;*
c) *rotation and uniform stretching while maintaining angles;*
d) *general rotation and stretching.*

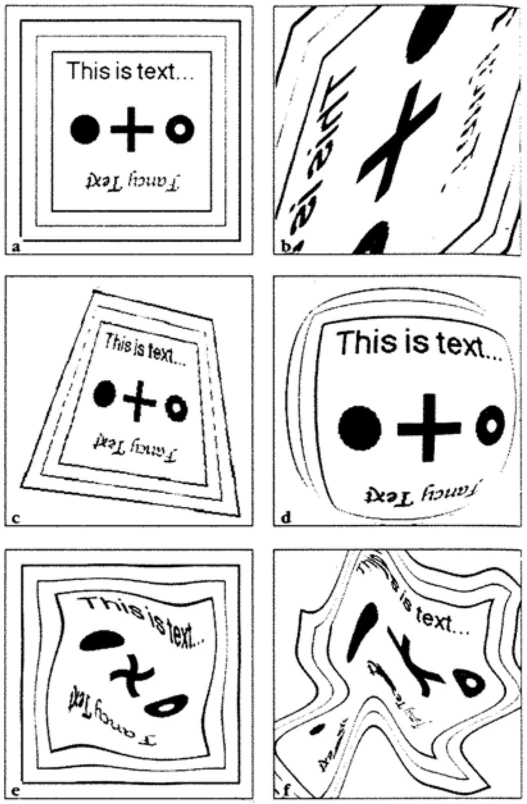

Figure 49. Some additional examples of image warping:
a) *original test image;*
b) *linear warping with reversal;*
c) *quadratic warping showing trapezoidal foreshortening (no interpolation);*
d) *cubic warping in which lines are curved (approximation here is to a spherical surface);*
e) *twisting the center of the field while holding the edges fixed (also cubic warping);*
f) *arbitrary warping in which higher order and trigonometric terms are required.*

Image Types

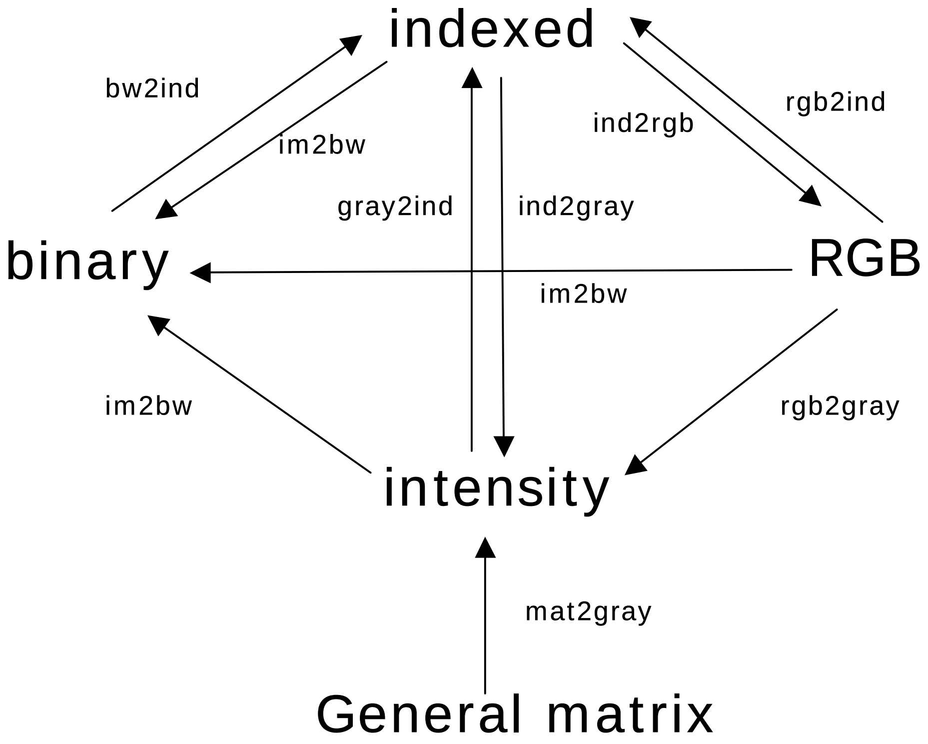

indexed

bw2ind

im2bw

ind2rgb

rgb2ind

gray2ind

ind2gray

binary

RGB

im2bw

im2bw

rgb2gray

intensity

mat2gray

General matrix

Histograms

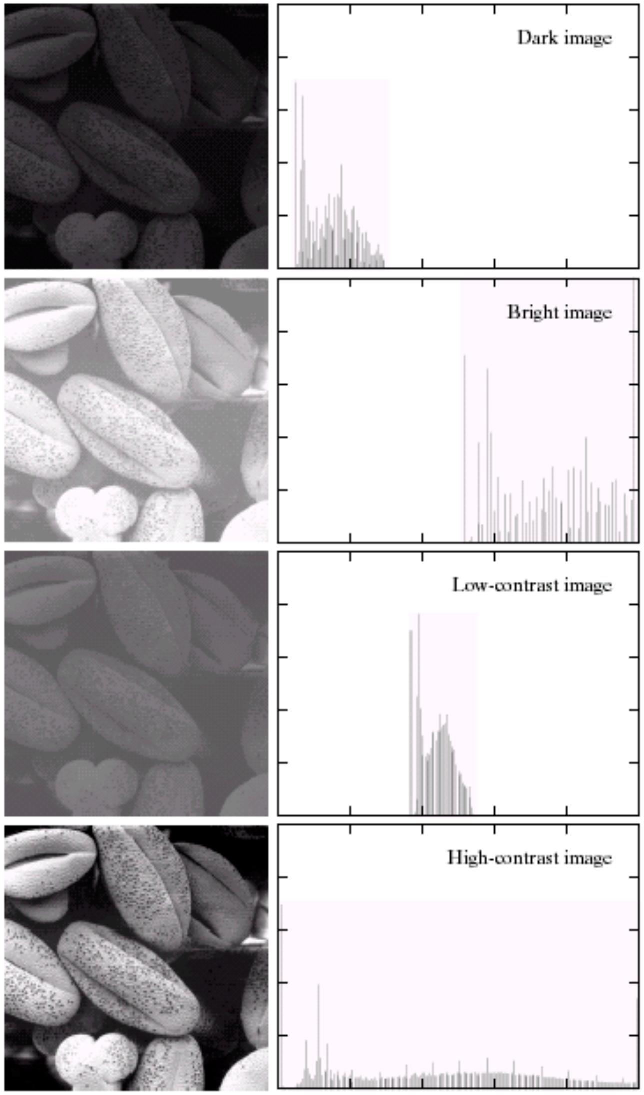
Dark image
Bright image
Low-contrast image
High-contrast image

Intensity Transforms (Contrast Enhancement)

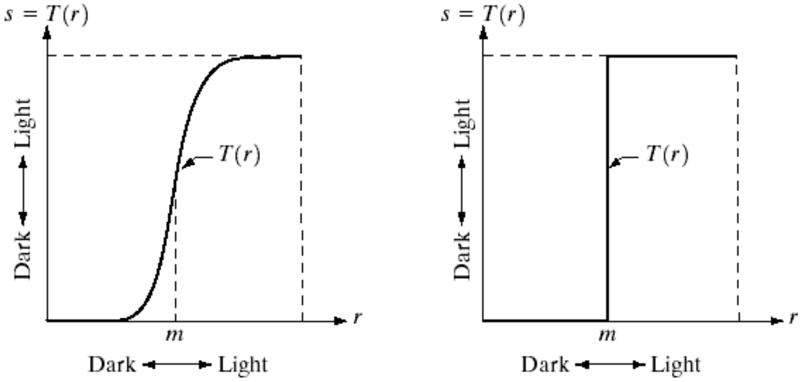

a b

FIGURE 3.2 Gray-level transformation functions for contrast enhancement.

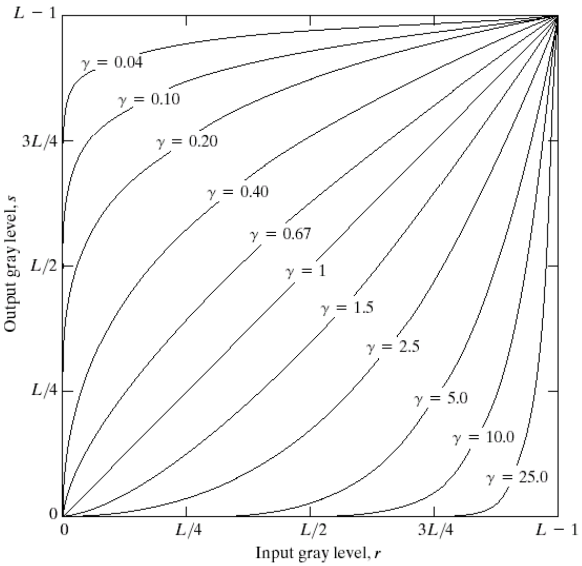

FIGURE 3.6 Plots of the equation $s = cr^{\gamma}$ for various values of γ ($c = 1$ in all cases).

Contrast Enhancement

a b
c d

FIGURE 3.9 (a) Aerial image. (b)–(d) Results of applying the transformation in Eq. (3.2-3) with $c = 1$ and $\gamma = 3.0, 4.0$, and 5.0, respectively. (Original image for this example courtesy of NASA.)

Histogram Equalization

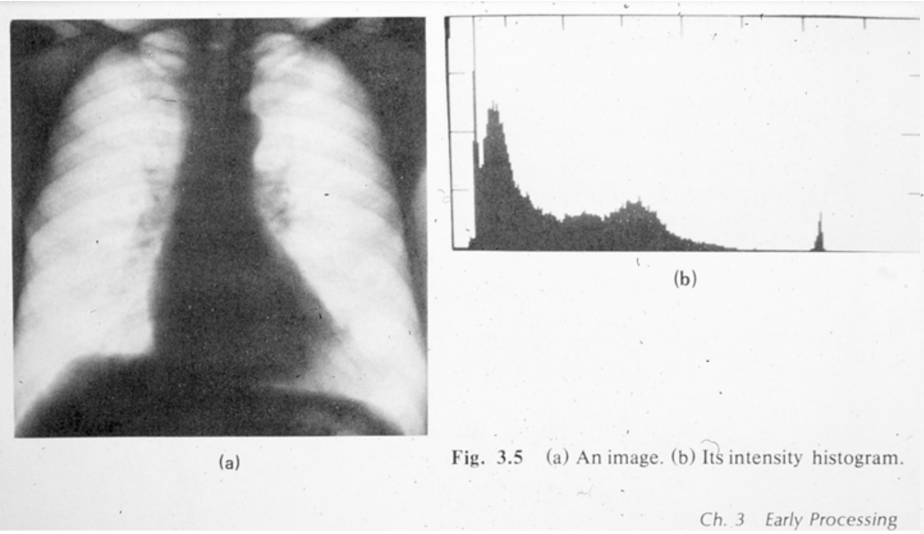
(a)

(b)

Fig. 3.5 (a) An image. (b) Its intensity histogram.

Ch. 3 Early Processing

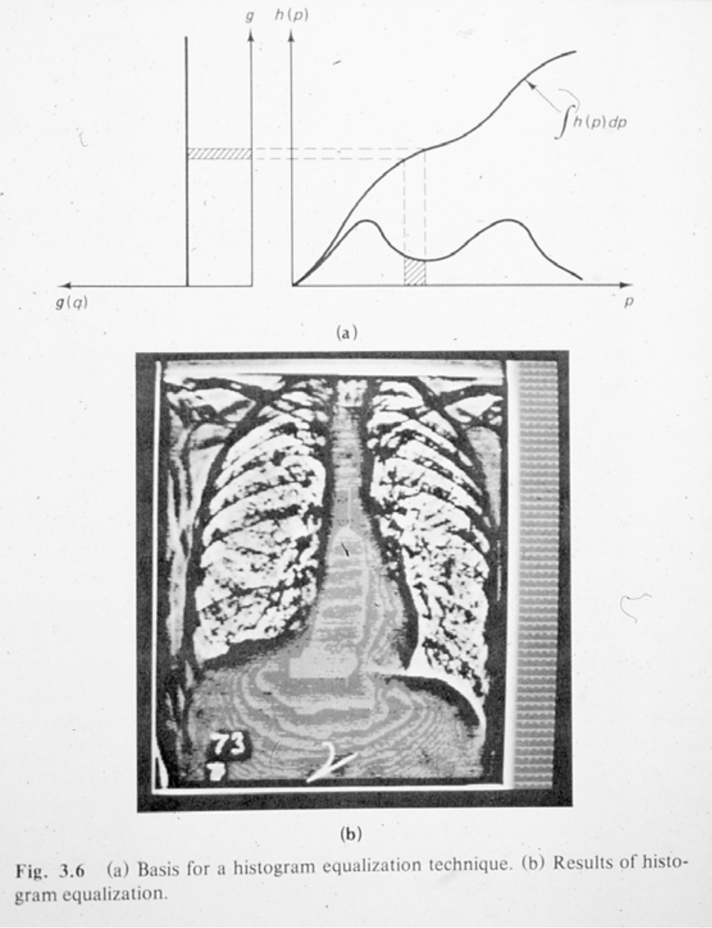

(a)

(b)

Fig. 3.6 (a) Basis for a histogram equalization technique. (b) Results of histogram equalization.

More Histogram Equalization

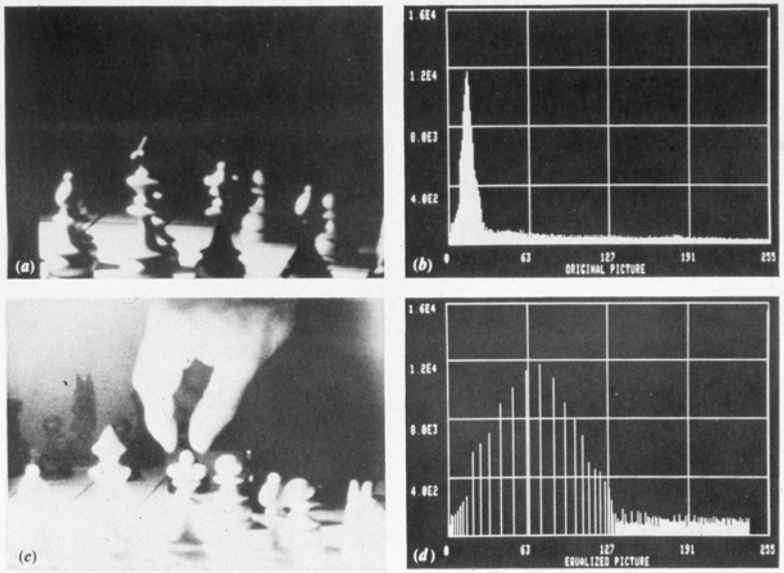

Figure 7.30 (*a*) Original image and (*b*) its histogram. (*c*) Histogram-equalized image and (*d*) its histogram. (From Woods and Gonzalez [1981], © IEEE.)

Histogram Equalization

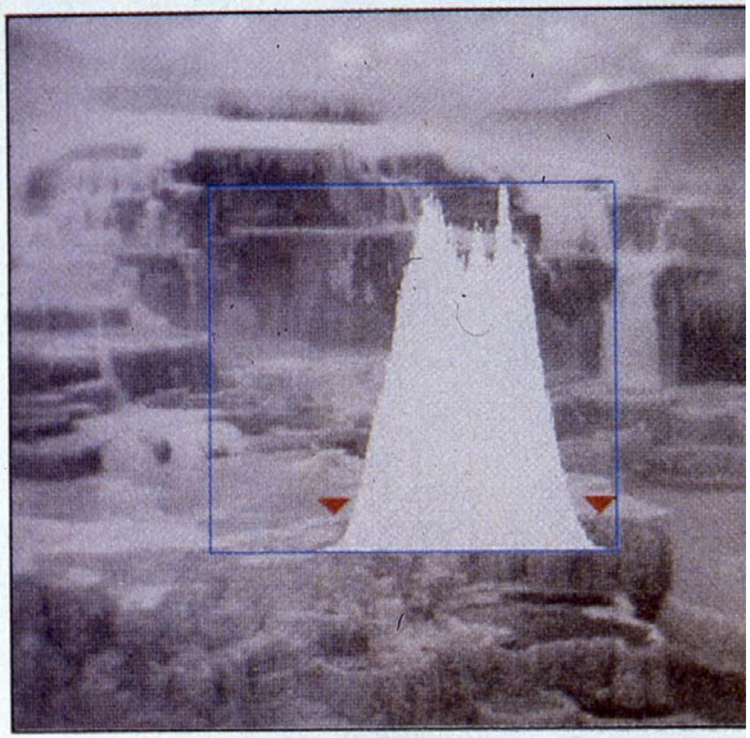

Photo 4: *An image of Athena's terrace in Yellowstone National Park overlaid with its histogram. Red arr indicate the lowest and highest ''bin as found by SIMPP's* clip__histo *routine.*

Photo 5: *Improved contrast of photo 4 results from histogram-based contrast stretching.*

Pseudocolor & LUTs

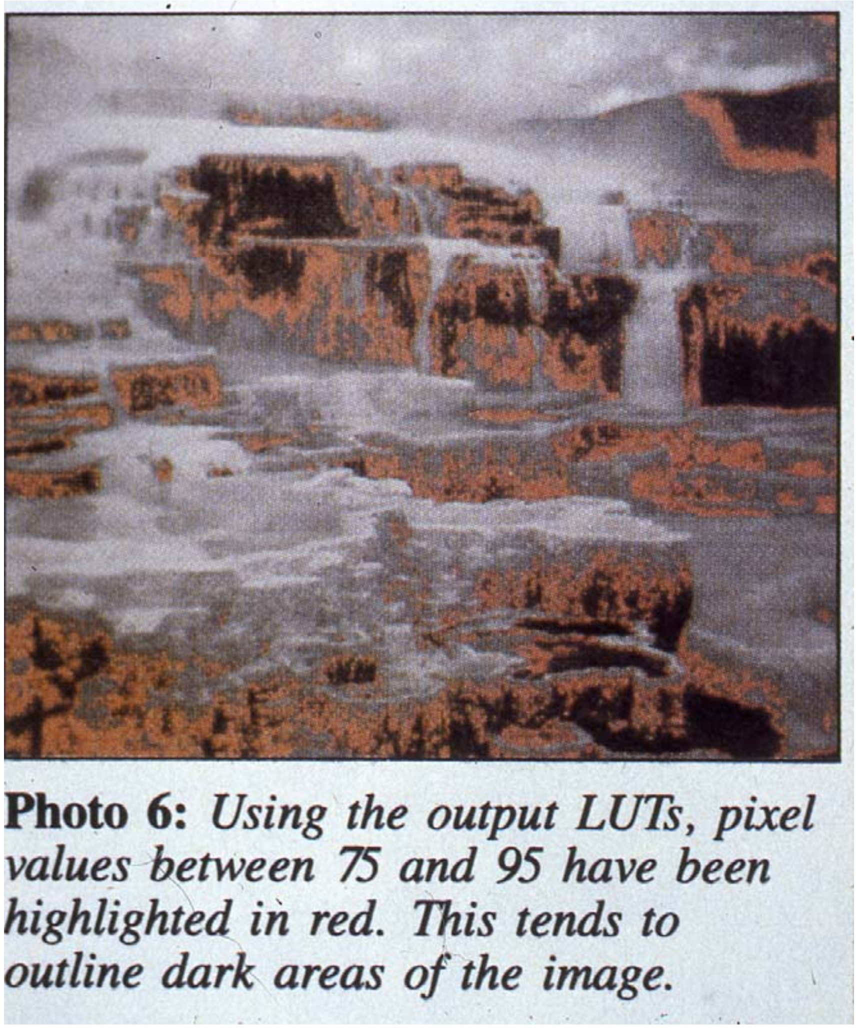

Photo 6: *Using the output LUTs, pixel values between 75 and 95 have been highlighted in red. This tends to outline dark areas of the image.*

Histogram Specification

Assume the histogram is represented by a probability density function $p_r(w)$

We can write the cumulative distribution function $s = T(r) = \int_0^r p_r(w)\,dw$

Define the distribution we want as $G(z) = \int_0^z p_z(t)\,dt$

What we do is simply set these two expressions equal $G(z) = T(r)$

Solve for the mapping from r to z, i.e., which can implicitly be solved to give

$$z = G^{-1}(s) = G^{-1}\left[T(r)\right]$$

While this can be implicitly solved in practice it is very difficult. However, it can readily be solved for discrete data.

Discrete Histogram Specification

a b
c

FIGURE 3.19 (a) Graphical interpretation of mapping from r_k to s_k via $T(r)$. (b) Mapping of z_q to its corresponding value v_q via $G(z)$. (c) Inverse mapping from s_k to its corresponding value of z_k.

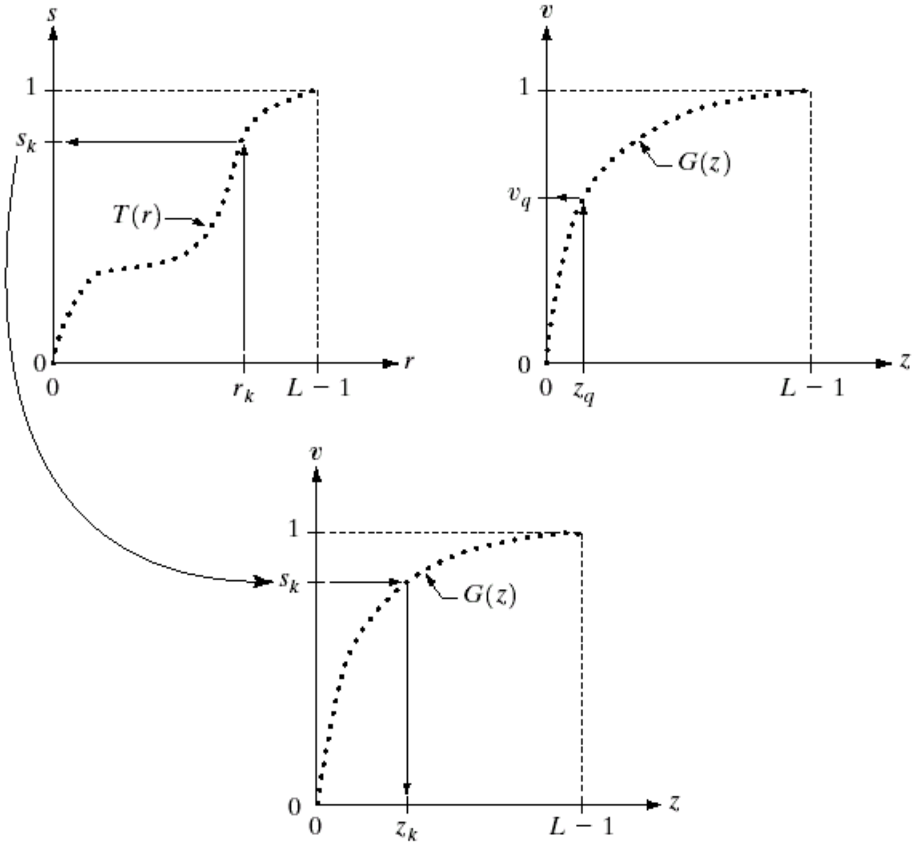

Histogram Specification

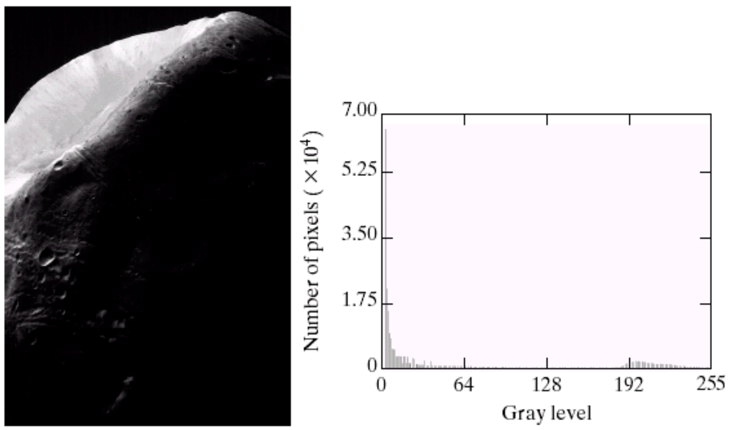

a b

FIGURE 3.20 (a) Image of the Mars moon Photos taken by NASA's *Mars Global Surveyor.* (b) Histogram. (Original image courtesy of NASA.)

a c
b
d

FIGURE 3.22
(a) Specified histogram.
(b) Curve (1) is from Eq. (3.3-14), using the histogram in (a); curve (2) was obtained using the iterative procedure in Eq. (3.3-17).
(c) Enhanced image using mappings from curve (2).
(d) Histogram of (c).

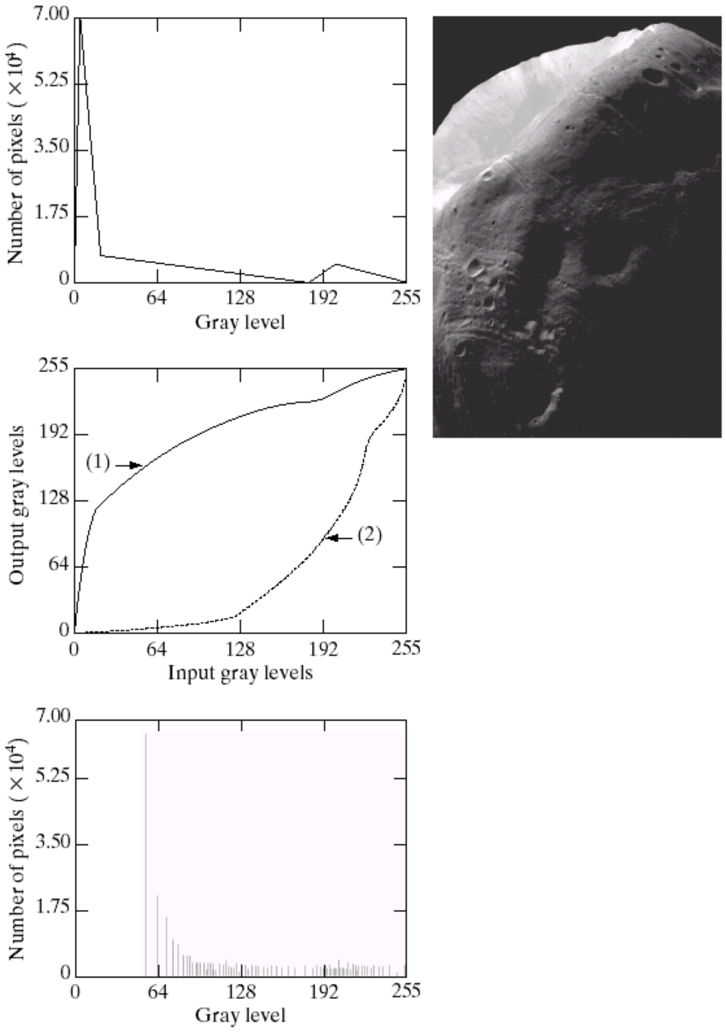

Selective Equalization

hoto 2: *An image of a bride, before age processing.*

Photo 3: *The result of modulating the contrast of photo 2 by a Gaussian curve, which provides an "aura" effect in the center.*